NASA CONTRACTOR
REPORT

N75-24856

NASA CR-61374

THE FABRICATION, TESTING AND DELIVERY OF BORON/EPOXY AND GRAPHITE/EPOXY NONDESTRUCTIVE TEST STANDARDS

By W. M. Pless and W. H. Lewis
Lockheed-Georgia Company
A Division of Lockheed Aircraft Corporation
Marietta, Georgia

December 1971

Final Report

Prepared for

NASA-GEORGE C. MARSHALL SPACE FLIGHT CENTER
Marshall Space Flight Center, Alabama 35812

1. Report No.	2. Government Accession No.	3. Recipient's Catalog No.
NASA CR-61374		

4. Title and Subtitle	5. Report Date
THE FABRICATION, TESTING AND DELIVERY OF BORON / EPOXY AND GRAPHITE / EPOXY NONDESTRUCTIVE TEST STANDARDS	December 1971
	6. Performing Organization Code

7. Author(s)	8. Performing Organization Report No.
W. M. Pless and W. H. Lewis	ER-11199
	10. Work Unit No.

9. Performing Organization Name and Address	11. Contract or Grant No.
Lockheed-Georgia Company A Division of Lockheed Aircraft Corporation Marietta, Georgia	NAS 8-27565
	13. Type of Report and Period Covered
12. Sponsoring Agency Name and Address	NASA Contractor Report
National Aeronautics and Space Administration Washington, D. C. 20546	14. Sponsoring Agency Code

15. Supplementary Notes

16. Abstract

This report describes the boron/epoxy and graphite/epoxy Nondestructive Test Standards which were fabricated and tested during this program and delivered to the George C. Marshall Space Flight Center, National Aeronautics and Space Administration. Detailed design drawings of the standards are included to show the general structure and the types and location or simulated defects built into the panels. The panels were laminates with plies laid up in the 0°, $\pm 45^\circ$, and 90° orientations and containing either titanium substrates or interlayered titanium perforated shims. Panel thickness was incrementally stepped from 2.36 mm (0.093 in.) to 12.7 mm (0.500 in.) for the graphite/epoxy standards, and from 2.36 mm (0.093 in.) to 6.35 mm (0.250 in.) for the boron/epoxy standards except for the panels with interlayered shims which were 2.9 mm (0.113 in.) maximum thickness. The panel internal conditions included defect-free regions, resin variations, density/porosity variations, cure variations, delaminations/disbonds at substrate bondlines and between layers, inclusions and interlayered shims.

Ultrasonic pulse echo C-scan and low-kilovoltage X-ray techniques were used to evaluate and verify the internal conditions of the panels.

17. Key Words (Suggested by Author(s))	18. Distribution Statement
	Unclassified-unlimited

19. Security Classif. (of this report)	20. Security Classif. (of this page)	21. No. of Pages	22. Price*
Unclassified	Unclassified	70	$3.00

*For sale by the National Technical Information Service, Springfield, Virginia 22151

Page Intentionally Left Blank

FOREWORD

Under Contract NAS8-27565, the Lockheed-Georgia Company fabricated, tested and delivered advanced composite standards according to designs submitted in RFQ No. 1-1-60-00302 from the George C. Marshall Space Flight Center, National Aeronautics and Space Administration, dated 19 April 1971. This final report presents the detailed designs, complete fabrication procedures, and the ultrasonic and radiographic evaluations of the test standards. For internal control purposes, this report has been designated as Lockheed-Georgia Report ER-11199.

This program was conductea in the General Structures and Materials Laboratory under the surveillance of Mr. D. G. Cumro, Manager of the Laboratory, and Mr. I. Capelouto, Manager of the Structural and Materials Laboratory. Mr. W. H. Lewis, Group Engineer of the Physical Test Group, was the Program Supervisor and Messrs. B. L. Weil and W. M. Pless were Principal Investigators.

The authors wish to acknowledge the important contributions made to this program by Mr. Fred Humphrey of the Physical Test Group, who was responsible for fabricating and curing the test standards.

TABLE OF CONTENTS

	Page
FIGURE INDEX	v
I - INTRODUCTION	1
II - DESIGN AND FABRICATION	2
o Design of Standards	2
o Fabrication of Standards	2
- Density/Porosity and Resin Variations	4
- Cure Variations and Inclusions	4
- Interlayered Titanium Shims	5
- Disbonds and Delaminations	5
o Fabrication Pictorial Summary	6
III - NONDESTRUCTIVE EVALUATION	7
o Ultrasonic Evaluation Technique	7
o Radiographic Evaluation Technique	8
o Nondestructive Evaluation Results	9
o Summary of Nondestructive Evaluation	13
ABSTRACTS	14
FIGURES	17
APPENDIX	A-1

FIGURE INDEX

Number	Title	Page
1.	Method of Cutting Prepreg Boron/Epoxy Tapes and Graphite/Epoxy Sheets.	18
2.	Hand Lay-up of a Typical Panel.	19
3.	Use of Caul Plate to Mold Panel Thickness Steps.	20
4.	Front and Back Faces of a Typical Panel.	21
5.	Perforated Titanium Shims used in Two of the Panels.	22
6.	All Finished Panels Ready for Shipment.	23
7.	Block Diagram of Ultrasonic C-scan Inspection System.	24
8.	Ultrasonic C-scan of Graphite/Epoxy Density/Porosity & Resin Variation Panel, Thickness A.	25
9.	Radiograph C-scan of Graphite/Epoxy Density/Porosity & Resin Variation Panel, Thickness A, Plain Areas. Exposure 45 Seconds.	26
10.	Radiograph of Graphite/Epoxy Density/Porosity & Resin Variation Panel, Thickness A, Substrate Areas. Exposure 2 Minutes.	27
11.	Ultrasonic C-scan of Graphite/Epoxy Density/Porosity & Resin Variation Panel, Thickness B.	28
12.	Radiograph of Graphite/Epoxy Density/Porosity & Resin Variation Panel, Thickness B, Plain Areas. Exposure 60 Seconds.	29
13.	Radiograph of Graphite/Epoxy Density/Porosity & Resin Variation Panel, Thickness B, Substrate Areas. Exposure 2 Minutes.	30
14.	Ultrasonic C-scan of Boron/Epoxy Density/Porosity & Resin Variation Panel.	31
15.	Radiograph of Boron/Epoxy Density/Porosity & Resin Variation Panel, Plain Areas. Exposure 2.5 Minutes.	32

FIGURE INDEX (con'd)

Number	Title	Page
16.	Radiograph of Boron/Epoxy Density/Porosity & Resin Variation Panel, Substrate Areas. Exposure 5 Minutes.	33
17.	Ultrasonic C-scan of Graphite/Epoxy Cure Variations and Inclusions Panel, Thickness A.	34
18.	Radiograph of Graphite/Epoxy Cure Variations and Inclusions Panel, Thickness A, Plain Areas. Exposure 30 Seconds.	35
19.	Radiograph of Graphite/Epoxy Cure Variations and Inclusions Panel, Thickness A, Substrate Areas. Exposure 3 Minutes.	36
20.	Ultrasonic C-scan of Graphite/Epoxy Cure Variations and Inclusions Panel, Thickness B.	37
21.	Radiograph of Graphite/Epoxy Cure Variations and Inclusions Panel, Thickness B, Plain Areas. Exposure 60 Seconds.	38
22.	Radiograph of Graphite/Epoxy Cure Variations and Inclusions Panel, Thickness B, Substrate Areas. Exposure 3 Minutes.	39
23.	Ultrasonic C-scan of Boron/Epoxy Cure Variations and Inclusions Panel.	40
24.	Radiograph of Boron/Epoxy Cure Variations and Inclusions Panel, Plain Areas. Exposure 2.5 Minutes.	41
25.	Radiograph of Boron/Epoxy Cure Variations and Inclusions Panel, Substrate Areas. Exposure 5 Minutes.	42
26.	Ultrasonic C-scan of Graphite/Epoxy Interlayered Titanium Shim Panel.	43
27.	Radiograph of Graphite/Epoxy Interlayered Titanium Shim Panel. Exposure 30 Seconds.	44
28.	Ultrasonic C-scan of Boron/Epoxy Interlayered Titanium Shim Panel.	45
29.	Radiograph of Boron/Epoxy Interlayered Titanium Shim Panel. Exposure 2.5 Minutes.	46

FIGURE INDEX (con'd)

Number	Title	Page
30.	Ultrasonic C-scan of Graphite/Epoxy Delaminations and Disbond Panel, Thickness A.	47
31.	Radiograph of Graphite/Epoxy Delaminations and Disbond Panel, Thickness A, Plain Areas. Exposure 45 Seconds.	48
32.	Radiograph of Graphite/Epoxy Delaminations and Disbond Panel, Thickness A, Substrate Areas. Exposure 3 Minutes.	49
33.	Ultrasonic C-scan of Graphite/Epoxy Delaminations and Disbond Panel, Thickness B.	50
34.	Radiograph of Graphite/Epoxy Delaminations and Disbonds Panel, Thickness B, Plain Areas. Exposure 60 Seconds.	51
35.	Radiograph of Graphite/Epoxy Delaminations and Disbonds Panel, Thickness B, Substrate Areas. Exposure 3 Minutes.	52
36.	Ultrasonic C-scan of Boron/Epoxy Delaminations and Disbonds Panel.	53
37.	Radiograph of Boron/Epoxy Delaminations and Disbonds Panel, Plain Areas. Exposure 2.5 Minutes.	54
38.	Radiograph of Boron/Epoxy Delaminations and Disbonds Panel, Substrate Areas. Exposure 5 Minutes.	55
A-1.	Design Drawing of the Density/Porosity and Resin Variations Panels.	A-2
A-2.	Design Drawing of the Cure Variations and Inclusions Panels.	A-3
A-3.	Design Drawing of the Interlayered Shim Panels.	A-4
A-4.	Design Drawing of the Perforated Titanium Shims.	A-5
A-5.	Design Drawing of the Delaminations and Disbonds Panels.	A-6
A-6.	Photograph of the Ultrasonic, C-scan System.	A-7
A-7.	Photograph of the Radifluor X-ray Cabinet.	A-8

I - INTRODUCTION

Designs for future space vehicles and hypersonic aircraft will specify the use of filamentary composite structures wherever possible because of their high modulus and high strength-to-weight ratios. Structures using graphite or boron filaments incorporated into plastic matrices are already proving their worth as improved, advanced materials applications on high-performance aircraft. Because of their relatively advantageous properties, these materials will displace considerable metallic components on future air and space vehicles.

Usage will be restricted in critical applications unless material properties can be reliably determined during fabrication and verified throughout the service life. The answer to this problem lies in the development and extensive use of improved nondestructive evaluation procedures and test equipment, which will require preparation of test standards adequate to determine material properties and discontinuities as a function of equipment response. Composite materials have many inherent variations not found in homogeneous metallic materials. The fabrication, testing, and use of filamentary composite structures will demand greater scrutiny through nondestructive evaluation than is presently provided for the less complex metallic structures.

The work reported herein was undertaken to provide the National Aeronautics and Space Administration with boron/epoxy and graphite/epoxy nondestructive test standards for evaluating materials on anticipated space vehicles. In design development ot the standards, consideration has gone beyond the detection of cracks and voids, into evaluation of other properties. The developed standards contain typical errors of fabrication and process peculiar to the chosen materials and processes so that the internal conditions of the standards represent the most probable conditions to be found in production hardware. The standards were fabricated by hand lay-up techniques, cured in an autoclave using a caul plate and rubber dam molding apparatus, followed by bonding on the titanium sheet substrates. The panels were then subjected to visual, radiographic and ultrasonic C-scan evaluation to determine the overall quality and conformance to design.

II - DESIGN AND FABRICATION

Design of Standards

The composite standards were designed to represent the material specifications of anticipated space vehicle structures as well as to incorporate typical fabrication and process errors leading to defective conditions. The types of defects were chosen to represent deviations from fabrication and process specifications, but all are not necessarily detectable by optimized state-of-the-art NDT equipment. To design for complete detectability would have limited the potential usefulness of the standards.

The detailed designs for fabrication of the standards were supplied by the NASA-MSFC. Boron/epoxy and graphite/epoxy standards were called for in two basic design configurations using either titanium substrates or interlayered titanium foil shims. The complete design drawings and specifications are presented in the Appendix in Figures A-1 through A-5.

Fabrication of Standards

General

The NDT composite standards were fabricated in the facilities of the Lockheed-Georgia General Structures and Materials Laboratory using typical production equipment. The standard panel size for both design configurations is 305 mm (12 inches) square. One configuration consists of two sets of laminates on titanium substrates having stepped thicknesses in two thickness ranges: (1) thickness range A: steps of 2.36 mm (0.093 in.), 3.17 mm (0.125 in.), 4.75 mm (0.187 in.), and 6.35 mm (0.250 in.); (2) thickness range B: steps of 7.94 mm (0.312 in.), 9.53 mm (0.375 in.), 11.1 mm (0.437 in.), and 12.7 mm (0.500 in.). The final thicknesses vary from these figures because of the unavoidable uncertainty in predicting accurately the thickness of a finished layed-up structure sans machining. Panel thicknesses are based on incremental thicknesses of 0.15 mm (0.006 in.) per ply for the graphite material and 0.18 mm (0.007 in.) for the boron material. The stepped thicknesses are spaced 76 mm (3 in.) apart. Machined coul plates were used during the cure cycle to assure definition of the steps.

The second configuration is a 15-ply laminate with interlayered perforated titanium shims. These shims, annealed Ti-6Al-4V Type III titanium foil 0.18 mm (0.007 in.) thick, are perforated by 1.6 mm (0.063 in.) diameter holes in rows spaced 6.14 mm (0.240 in.) apart. The original shim design is shown in Figure A-4.

The graphite panels were made from Lockheed LLM graphite fibers prepregged with Ciba DLS-77 epoxy resin (equivalent to Whittaker 5205, Type-2 Morganite), which is produced in 305 mm (12 in.) by 965 mm (38 in.) sheets. The boron panels were made from Whittaker Rigidite 5505 boron/epoxy tapes approximately 76 mm (3 in.) wide. The graphite material is produced in configurations of 1.56 tows per cm (four tows per inch).

The prepreg materials were layed up so as to produce 0°, -45°, 90°, and $+45^{\circ}$ orientations throughout each panel. The panels were molded in a clam shell autoclave at 5.98 kg/cm^2 (85 psig) for 60 minutes at $177^{\circ}C \pm 5^{\circ}C$ ($350^{\circ}F, \pm 10^{\circ}F$) for graphite, 3.46 kg/cm^2 (50 psig) for 2 hours for boron. The time and temperature exposures for the cure variation panels varied from the above while in the autoclave. Panel size and thickness were controlled by the use of closed silicone rubber dams and controlled bleeding techniques. Titanium sheet metal strips 0.5 mm (0.020 in.) thick were bonded to the laminates in a secondary bonding operation using HySol 9614 adhesive cured at $66^{\circ}C$ ($150^{\circ}F$) for two hours.

The internal defects were placed in the laminates between the 9th and 10th plies at the time of lay-up. Other defects were incorporated during the cure process or prior to the secondary bonding operation.

The following defect conditions were molded into the panels:

	Number of Panels	
	Boron	Graphite
Density/porosity & Resin Variation	1	2
Cure Variations & Inclusions	1	2
Interlayered Titanium Shims with adhesive voids at 2nd & 4th shims	1	1
Delaminations/Disbonds	1	2
Total	4	7

The boron panels consisted only of the 'A' thickness range, as described earlier, and the graphite panels consisted of both 'A' and 'B' thickness ranges. Defect-free areas exist in all panels.

Density/Porosity and Resin Variations

Two graphite/epoxy and one boron/epoxy panels contain density, porosity and resin variations. The density variation is actually a result of varying the amount of internal porosity and the amount of resin bleed-off allowed while curing the panels. Porous conditions were achieved in Regions A and D of the panels by inserting phenolic microballoons (Eccospheres) between plies 9 and 10. The size of the spheres were less than 1.52 mm (0.06 inch) diameter, determined by selecting spheres which passed through a #12 mesh screen. Achieving porosity by reduced pressure in specific areas during cure was not successful and this approach had to be abandoned.

Resin-rich and resin-poor areas characterizing each half of the panel were achieved through a controlled bleeding technique using Mylar and Armalon separately on halves of the laminates. The pre-preg tapes exhibit a resin variation of $\pm$ 3% of the nominal specified value which can contribute to normal variations in defect-free regions of the finished laminate. The percent resin content for a finished 5505 boron laminate is nominally 23.5 and for a finished LLM graphite laminate is nominally 30.5.

Cure Variation and Inclusion

It was desired to produce a state of undercure in two graphite panels and one boron panel to represent an understrength condition in these panels. An unsuccessful attempt was made to produce undercure in one-half of each panel by using an aluminum heat sink secured to the half of the panel and extending from the heated platen press at 182°C (360°F) for 60 minutes, followed by heating the entire panel in an oven of 154°C (310°F) for 30 minutes for the boron/epoxy laminate and 120°C (248°F) for 40 minutes for the graphite/epoxy laminate. This procedure produced a poor quality panel with uncontrollable warpage and gross thickness variations. It was decided that a panel having half undercure and half proper cure could not be reliably produced and that the entire panel should be left in a state of undercure. This

was achieved by curing the panels in the autoclave at 154°C (310°F) for 30 minutes for the boron/epoxy laminate, 107°C (225°F) for 30 minutes for the graphite/epoxy thickness 'A' laminate, 113°C (235°F) for 30 minutes for the graphite/epoxy thickness 'B' laminate.

A strip of prepreg backing -- a typically occurring inclusion resulting from careless lay-up -- was incorporated into each of these panels in Region F, which is partially overlapped by the titanium sheet substrate.

Interlayered Titanium Shims

Two laminates containing perforated titanium shims were fabricated -- one each of boron/epoxy and graphite/epoxy. Each panel contains five shims which were incorporated into the 15-ply laminate as illustrated in Figure A-3. Narmco 2387 adhesive was applied at the ends of shims 1, 3 and 5 to eliminate voids at these points. No adhesive was applied at the ends of shims 2 and 4. The shims were made of annealed Ti-6Al-4V titanium Type III foil 0.18 mm (0.007 in.) thick which were perforated with 1.6 mm (0.063 in.) diameter holes arranged in rows spaced 6.14 mm (0.240 in.) apart. Before laying these panels up, the titanium shims were treated with Pasa-Jell 107-M, MFGR Code 83574. During lay-up the shims were butted against a rigid guide to obtain alignment.

Delaminations and Disbonds

Delaminations and disbonds were simulated in two graphite/epoxy panels and one boron/epoxy panel by inserting discs of Tedlar or Armalon at the locations specified in Figure A-5. Discs of 12.7 mm (0.50 in.) diameter were inserted between the 9th and 10th plies in all thickness steps in the substrated area and in the unsubstrated area. Smaller discs of 6.4 mm (0.250 in.) diameter were also inserted in the unsubstrated area between the 9th and 10th plies. To simulate disbonds between the titanium substrate and adhesive, 12.7 mm (0.50 in.) diameter Tedlar/Armalon discs were inserted on each thickness step. Gross delamination from overaged material was produced by pre-staging strips of prepreg tape in an oven at 135°C (275°F) for four hours to simulate 60 days out of refrigeration. These strips were inserted as the 9th and 10th plies at position R_L-R_{LT}.

Fabrication Pictorial Summary

Figure 1 indicates the procedure for cutting the prepreg tapes after measuring for proper length and orientation. The boron/epoxy disbond panel is shown in the process of lay-up in Figure 2. The Tedlar/Armalon inserts are shown being placed on the 10th layer, after which the 9th layer will be placed down. The tape joints and the method of laying-up the panels on the caul plate can be easily seen.

Figure 3 shows how the caul plate was used to mold the thickness steps into a typical panel. A finished density/porosity panel is shown in Figure 4, complete with titanium substrates. A photograph of two perforated titanium foil shims is shown in Figure 5.

The complete array of the eleven graphite/epoxy and boron/epoxy composite standards is shown in Figure 6, photographed just prior to shipment to NASA-MSFC.

III - NONDESTRUCTIVE EVALUATION

To verify the quality and simulated defective conditions of the composite standards, each panel was subjected to nondestructive evaluation utilizing radiographic and ultrasonic C-scan techniques. In filamentary composites, both NDT methods are needed to adequately evaluate the material. Not all material conditions are observable with state-of-the-art NDT techniques, although some of these are physically possible. Conditions such as state-of-cure may be observable through the measurement of ultrasonic velocity, but some means must be used to account for measurement perturbations arising from intrinsic material variability. This separation of variables will require techniques not presently in common use in the field of nondestructive evaluation.

In general, material variables such as filament population variations, tape butt joints, and geometric edges tend to interfere with the observation of defects and structural characteristics in NDT graphic records. This is particularly true with the boron/epoxy panels and is more pronounced with the ultrasonic technique than with radiography. Scattering and differences in attenuation of ultrasound occurring with these conditions are often the most pronounced effects produced in the NDT graphic recordings. In radiography, the boron/tungsten filaments which have greater density than the surrounding epoxy matrix may mask the defect simulation, particularly the Tedlar/Armalon discs and the phenolic microballoons. With the complementary nature of these two NDT methods, it was often possible to verify a defect condition with one technique which was not observable with the other technique. In other cases, defects are observable with both techniques.

The Ultrasonic Technique

A pulse-echo C-scan technique was employed, characterized by a focussed ultrasonic beam, water immersion, and an aluminum reflector plate. The ultrasonic system consisted of a Sperry UM-721 Reflectoscope; Sperry UM-710 Special Function Cabinet containing a Transigraph, Fast Transigate, and a Type "S" Recording Amplifier; Automation Industries Research Tank containing a scanning/indexing bridge, the water-immersion tank, and an Alden Type 311DA Alfax Recorder. Figure 7 shows a functional block diagram of this system, while Figure A-6 is a

photograph of the system. An Automation Industries Type SIZ/5.0 MHz/9.5 mm (0.375-inch) diameter/sharp-focus search unit, Style 57A3620, was used as transmitter and receiver throughout. The search unit was pulsed at 5 MHz. This frequency gave the best, most consistent results for each type of panel. Some advantage in transmissibility was evident at 2.25 MHz, but resolution was sacrificed at this lower frequency.

While obtaining the C-scan recordings the composite panel was positioned 5.08 mm (0.200 in.) above a flat, smooth aluminum plate which served to reflect the signal after passing through the panel. The returned signal retraced its path through the panel and was received by the transducer. The Fast Transigate was gated to pass this signal onto the recording amplifier. The upper and lower voltage limits on the Transigraph were adjusted to provide good contrast for the overall conditions of each panel. Some recording enhancement can be achieved by optimizing the voltage limits for the conditions one wishes to observe.

In obtaining the recordings, it was necessary to adjust the receiver sensitivity for each thickness step on a panel. The areas containing the titanium substrate also required a different range of sensitivity. The search-unit-to-reflector path was maintained at 45 to 50 mm (1.75 to 2.0 inches).

The Radiographic Technique

All panels were radiographed in a laboratory X-ray cabinet -- the Radifluor 120 manufactured by the Torr X-ray Corporation shown in Figure A-7. The simplicity of this system permitted optimum radiographic parameters to be determined for each panel and maintained as necessary. All panels were radiographed at 120 KV, 5 ma. tube current, and 114.3 mm (45 inches) film-to-source distance. Once these parameters were determined, it was necessary to vary only the exposure time as required for each panel.

The radiographs were exposed on Agfa Type D-2 double-emulsion X-ray film which was subsequently developed in a Kodak X-omat automatic film processor. Generally, separate exposures were required for substrated and plain areas of each panel to obtain best results. Filament characteristics were plainly revealed in all boron/epoxy panels, but were considerably less noticeable in the graphite/epoxy panels since the components of the latter have nearly equal densities.

Nondestructive Evaluation Results

Density/Porosity and Resin Variations

Graphite - The ultrasonic C-scan recording of the graphite density/porosity panel, thickness "A", is shown in Figure 8. In this figure and all subsequent figures, the thinnest step of the panel is on the left side of the Figure, with increasing thickness toward the right. The notations shown on the C-scan recordings correspond to the notations given on the design drawings in the Appendix. In Figure 8, the porosity which was produced by the phenolic microballoons, appears as white dots in Sections A_{LT}, A_L, D_L, and D_{LT}. White dots in Regions B_{LT} and C_{LT} are attributed to the presence of graphite slag. Slag appeared in several of the panels, but once its presence was discovered steps were taken to minimize its occurrence in the remaining panels. The large blotch near the center of the recording is due to scattering of the ultrasound caused by slight exfoliation when the bleed cloth was removed from the backside of the panel. The condition is slight and its display on the recording is largely a matter of resolution and ultrasound beam geometry. The higher resin content in Regions C and D does tend to increase the ultrasound attenuation, tending to slightly lighten the C-scan recordings in these areas when the receiver sensitivity is more optimally adjusted. Figure 9 is a radiograph negative print of this same panel optimized for the plain areas, and Figure 10 is a radiograph print optimized for the substrated areas. The phenolic microballoons were easily seen in the original full-size radiographs. About 40 percent of the microballoons seem to have been crushed to some degree during curing under a pressure of 5.98 kg/cm^2 (85 psig). These radiographs were exposed for 45 seconds and 2 minutes, respectively.

Figure 11 is an ultrasonic C-scan recording of the graphite density/porosity panel, thickness "B". White dots in Regions A_{LT}, A_L, D_L, and D_{LT} result from the microballoons and represent the porous conditions. The higher resin content in Regions C and D has tended to produce a lightening of recording tone.

Figure 12 is a radiograph print of the plain areas of this panel, exposed for 60 seconds. Figure 13 is a radiograph print of the substrate areas, exposed for 2 minutes. The radiographs exhibited the microballoons in areas A_{LT}, A_L, D_L, and D_{LT}, showing that some were crushed under the pressure of cure.

Boron - An ultrasonic C-scan recording of the boron density/porosity panel is shown in Fig. 14. Porosity due to the microballoons appears in Regions A_{LT}, A_L, D_L, and D_{LT}. The greater variability produced in this recording (and recordings of other boron panels) by the larger and denser boron filaments and tape joints tends to obscure the evidence of porosity and resin variations. These effects can be reduced somewhat by pulsing the search unit at 2.25 MHz, although some resolution and sensitivity is thereby sacrificed.

Figures 15 and 16 are radiograph prints of the plain and substrate areas, respectively, of this boron panel. They were exposed for 2.5 minutes and 5 minutes, respectively. The microballoons could not be seen in these radiographs due to the filament images and because the need to expose the panel for long periods of time overexposed the film for viewing nonmetallic images.

Cure Variations and Inclusions

Graphite - Figure 17 shows the ultrasonic C-scan recording of the graphite cure variation/inclusion panel, thickness A. The cure variation/inclusion panels were given a uniform undercure condition over the entire panel, necessitating the detection of the undercure condition be made by comparing the NDT results with a properly cured panel. The backing inclusion in Regions F_{LT} and F_L is readily seen. Figures 18 and 19 show the radiograph prints for the plain and substrated areas of this panel. These radiographs, exposed for 30 seconds and 3 minutes, respectively, did not reveal the thin paper backing inclusion.

The ultrasonic C-scan recording for the graphite cure variation/inclusion panel, thickness "B", is shown in Figure 20. Again, the backing inclusion is visible in Regions F_{LT} and F_L. Figures 21 and 22 are the radiograph prints of the plain and substrate areas of the panel, exposed for 60 seconds and 3 minutes, respectively. The backing inclusion is not visible in the radiographs.

Boron - Figure 23 is the ultrasonic C-scan recording of the boron cure variation/inclusion panel. The backing inclusion is very pronounced in region F_{LT}. The inclusion in region F_L is less evident because the C-scan recording including this region was optimized for presenting the substrated area. A C-scan optimized for the plain areas clearly revealed the inclusion in

region F_L. Some general delamination seems to exist in the third thickness step of this panel as indicated by the light areas in the recording.

Figures 24 and 25 are the radiograph prints of the plain and substrate areas of this panel. They were exposed for 2.5 minutes and 5.0 minutes, respectively. Although filament orientation and features are observable in these figures, none of the defect conditions are visible.

Interlayered Titanium Shims

Graphite - The ultrasonic C-scan recording of the graphite-interlayered titanium shim panel is shown in Figure 26. A panel of this type requires a considerable difference in receiver sensitivity levels between the plain and shimmed areas. Considerable difficulty is thereby presented in properly characterizing the run-out regions of the shims in an optimized manner in order to expose the adhesive voids at the 2nd and 4th shims. A more optimized ultrasonic investigation of this region was precluded by a malfunction in a electromechanical indexing device in the scan/index system. However, the present C-scan indicates variability in the epoxy-titanium bonding in the shimmed area. The radiograph of this panel, shown in the print in Figure 27, shows that a slight amount of slippage occurred among some of the shims during cure. This radiograph was exposed for 30 seconds, causing the shimmed area to be underexposed, but sufficient to reveal shim features.

Boron - Figure 28 is an ultrasonic C-scan recording of the boron interlayered titanium shim panel. The same difficulty exists for this panel as for the graphite panel in characterizing the shim run-out region. A more properly adjusted instrument sensitivity while scanning this region indicates that the conditions which exist at the edges of the shims can be characterized. The "edge-effect" interferes with any such characterization, however. The epoxy-to-titanium bonding in this panel appears to be very uniform. Filament and shim features are produced in the C-scan recordings.

The radiograph print of the boron/shim panel is shown in Figure 29. The radiograph, exposed for 2.5 minutes, clearly shows the filament and shim features, but does not reveal adhesive voids at the edges of the 2nd and 4th shims.

Delaminations and Disbonds

Graphite - A ultrasonic C-scan recording of the graphite delaminations/disbonds panel, thickness A, is shown in Figure 30. All delaminations and disbonds caused by the Armalon/Tedlar inserts are revealed in each thickness step of this panel. An additional spreading delamination originates at and radiates from the N_{LT} delamination insert in the third thickness step. General delamination occurred due to the pre-aged strip in Regions R_{LT} and R_L.

The radiograph prints for the plain and substrate areas are shown in Figure 31 and 32, which were obtained at exposures of 45 seconds and 3 minutes, respectively. The Armalon/Tedlar inserts were visible in each radiograph, although the pre-aged strip did not produce any visible image. Also visible in the radiograph which produced Figure 32 are the traces of perturbed epoxy at the N_{LT} insert in the third thickness step, thus verifying the extended delamination at this location.

Figure 33 is an ultrasonic C-scan of the graphite delamination/disbond panel, thickness B. All delamination and disbond inserts and general delamination due to pre-aged material in Regions R_{LT} and R_L are clearly visible in this recording. The radiograph prints in Figures 34 and 35 are of the plain and substrate areas. The radiographs were exposed for 60 seconds and 3 minutes, respectively. The Armalon/Tedlar inserts are visible in the radiographs, although somewhat fainter images were produced than those revealed in the "A" panel radiographs. The images in the radiograph over the substrate area are very faint, but sufficient to verify the presence of the inserts.

Boron - Figure 36 is an ultrasonic C-scan recording of the boron delamination/disbond panel. All delaminations and disbonds arising from the Armalon/Tedlar inserts can be noted. General delamination due to the pre-aged strip is quite evident in Regions R_{LT} and R_L. Other light areas in Regions P and N_{LT} are apparently caused by variations in the bonding of the titanium strip to the composite panel. As with other boron panels, the filaments and tape joints produce scattering and attenuation which interferes with observing defect conditions.

The radiograph prints of the plain and substrate areas of this panel are shown in Figures 37 and 38. These radiographs were exposed for 2.5 minutes and 5 minutes, respectively. Although

filament and tape features are observable in the radiographs, the Armalon/Tedlar inserts are not visible. The long exposure times for these panels and the filament images prevent the inserts from being observable features in the radiographs.

Summary of Nondestructive Evaluation

Ultrasonic and radiographic nondestructive evaluation techniques have separately or in combination verified and/or indicated all design defect conditions with the exception of cure variation and adhesive voids at the titanium shim run-outs. Detection of the cure variations will depend on techniques not utilized in this program. Though some indication of adhesive voids existing at the shim runouts on the boron panel was obtained, clear revelation of the conditions existing in this region are very difficult to obtain due to edge effect and the need to compensate for rapid changes in attenuation due to the staggered shim edges.

General structural features and unintentional defect conditions were also revealed in the panels by these two NDE techniques. The two techniques can be optimized for the particular panel configuration to detect most of the defect conditions in the panels and to evaluate the effect of structural features on detection reliability.

ABSTRACTS OF SELECTED REPORTS

The following list of reports and articles, by no means exhaustive or optimum, will provide valuable information in evaluation of composites.

1. Anderson, R. T. and T. J. Delacy, "Application of Nondestructive Testing for Advanced Composites," Presented at March 1969 AFML/Aerospace/ University of Dayton Conference on NDT of Plastic/Composite Structures.

   ABSTRACT: This paper describes special radiographic and ultrasonic techniques applied to testing metal-matrix composites and other techniques applied to resin matrix composites. Approaches to display and analyze ultrasonic and radiographic data is presented. Methods using video filters, analog and digital computers for enhancing and displaying these data are described. Other NDT methods investigated include thermal gradient methods, eddy current and neutron radiography.

2. Lockyer, G. E., et al, "Investigation of Nondestructive Methods for the Evaluation of Graphite Materials, ' AFML-TR-67-128, June 1967.

   ABSTRACT: This technical report describes work performed under contract to the Air Force Materials Laboratory to verify and apply previously determined correlations between graphite materials properties and various NDT data. Primary emphasis is on an infrared method for measuring a thermal parameter of graphite materials. Of chief interest relative to the NASA composite standards is Part IV and Appendix II.

3. Martin, G., and J. F. Moore, "Research and Development of Nondestructive Testing Techniques for Composites," AFML-TR-66-270, February 1967.

   ABSTRACT: Reports on early investigations and development of nondestructive test methods for evaluating metal matrix composites. Ultrasonic, radiographic, and magnetic techniques are described for detecting

defects and evaluating internal structure of composite panels are described. A description of ultrasonic velocity measurements for determining material properties is presented.

4. Martin, G. and J. F. Moore, "Research and Development of Nondestructive Testing Techniques for Composites," AFML-TR-68-202, June 1968.

   ABSTRACT: Reports on optimization of ultrasonic and radiographic techniques developed in earlier program for evaluating metal matrix composites. Presents problems with material variability which must be overcome in development of adequate techniques. Electromagnetic, acoustic velocity and other nondestructive test techniques applied to metal matrix composites during the contract period are discussed.

5. Mool, D., and R. Stephenson, "Ultrasonic Inspection of a Boron/Epoxy - Aluminum Composite Panel," Materials Evaluation, July 1971, p. 159.

   ABSTRACT: This article describes nondestructive test techniques applied in quality control of composite compression members. An 11-ply boron/epoxy laminate sandwiched between two aluminum face-sheets containing simulated defects was used in determining feasibility of ultrasonic techniques to evaluate such materials. The test panel, test techniques and results are discussed.

6. Pless, W. M., B. L. Weil and W. H. Lewis, "Development, Fabrication, Testing, and Delivery of Advanced Filamentary Composite Nondestructive Test Standards," NASA Report N71-16595, Contract NAS8-25679, Lockheed-Georgia Report ER-10883, November 1970.

   ABSTRACT: This report describes the design, fabrication, and testing of graphite/epoxy and boron/epoxy composite test standards in flat panel and honeycomb configurations. The design drawings and complete fabrication information is presented. Destructive and nondestructive test results from ultrasonic and radiographic NDT techniques for determining panel quality and verifying design compliance are also presented.

7. Schultz, A. W., "The Development of Nondestructive Methods for the Quantitative Evaluation of Advanced Reinforced Plastic Composites," AFML-TR-70-20, August 1970.

ABSTRACT: This report documents a portion of a continuing study funded by AFML to investigate and determine the applicability of ultrasonic and radiometric techniques to predictive correlations with various physical properties of multi-oriented boron/epoxy panels, carbon/carbon panels, and quartz/phenolic spheres. Ultrasonic velocity, ultrasonic polar modulus, and gamma ray absorption values were measured to compare with elastic modulus, tensile, compression, flexure and shear modulus values of the materials.

8. Stinebring, R. C., and J. R. Zurbrick, "Properties Determination and Process Control of Boron Filament Composites Using Nondestructive Test Methods," Paper presented to the 10th National Symposium of Aerospace Material and Process Engineers, San Diego, California, Nov. 1966.

ABSTRACT: This paper describes the utilization of ultrasonic, radiographic, dye penetrant, and electric field techniques to measure, monitor and control variability in boron filament composites. The use of ultrasonic velocity measurements to predict shear strength and radiographic and dye penetrant methods to detect filament abnormalities and delaminations are described.

FIGURES

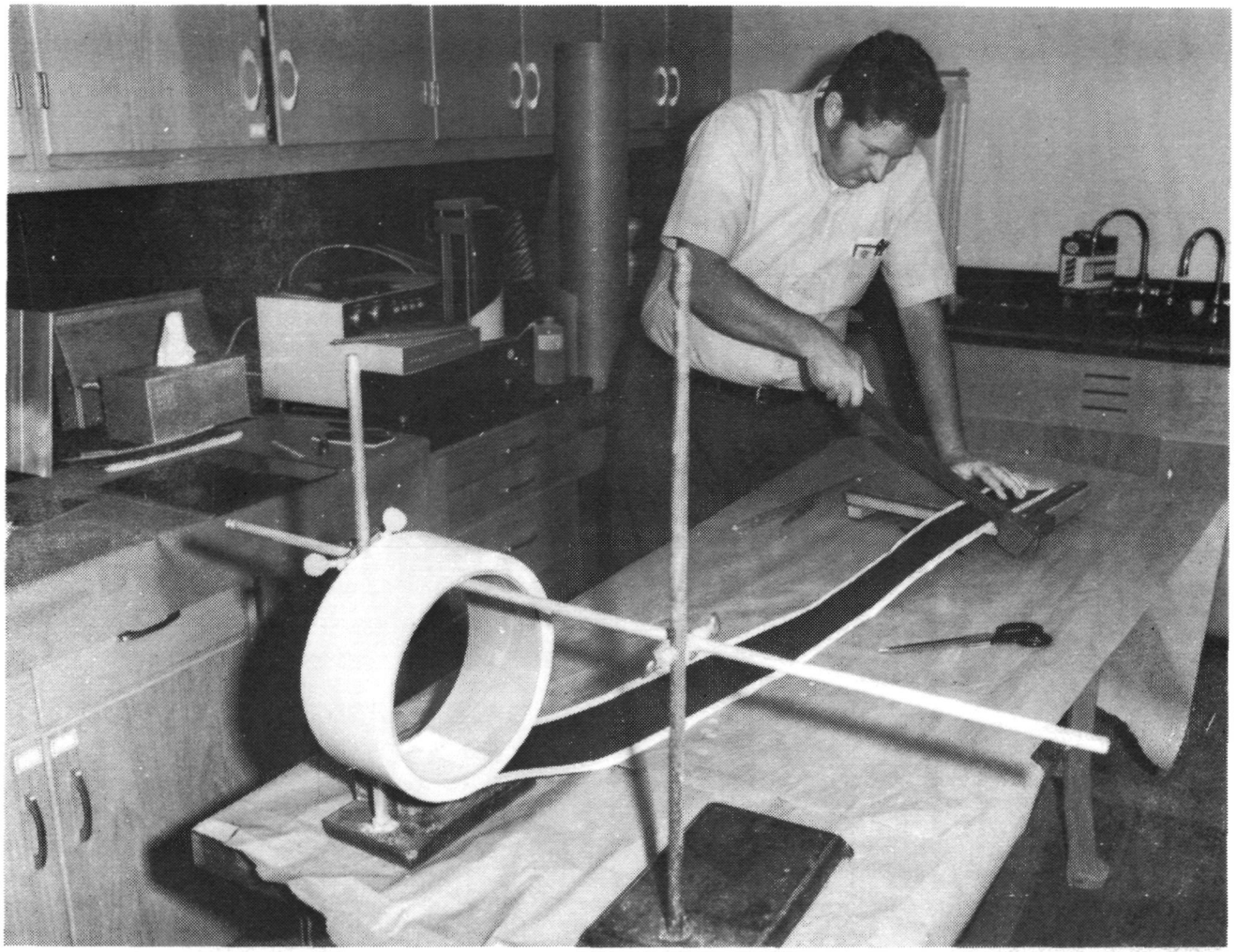

FIGURE 1. METHOD OF CUTTING PREPREG BORON/EPOXY TAPES AND GRAPHITE/EPOXY SHEETS.

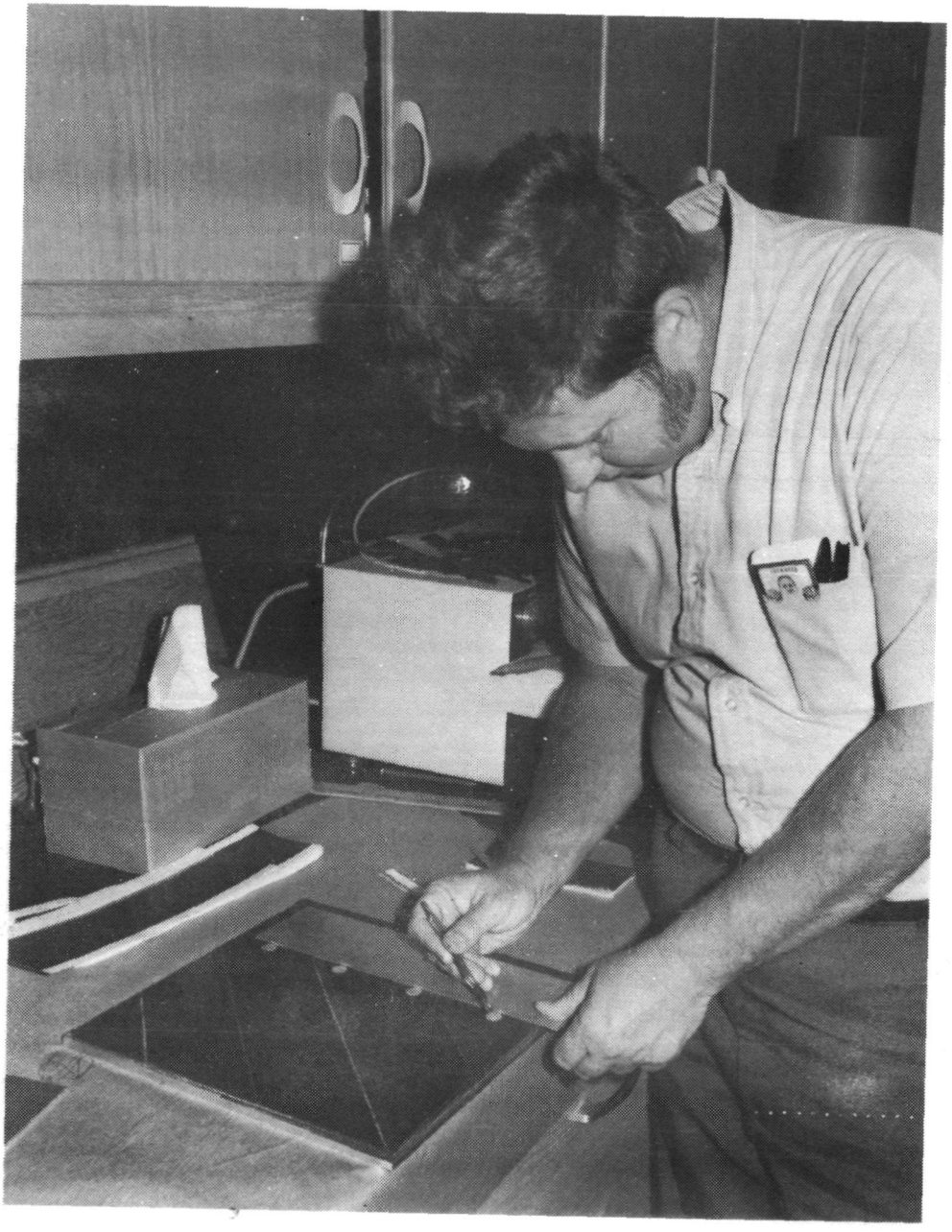

FIGURE 2. HAND LAY-UP OF A TYPICAL PANEL.

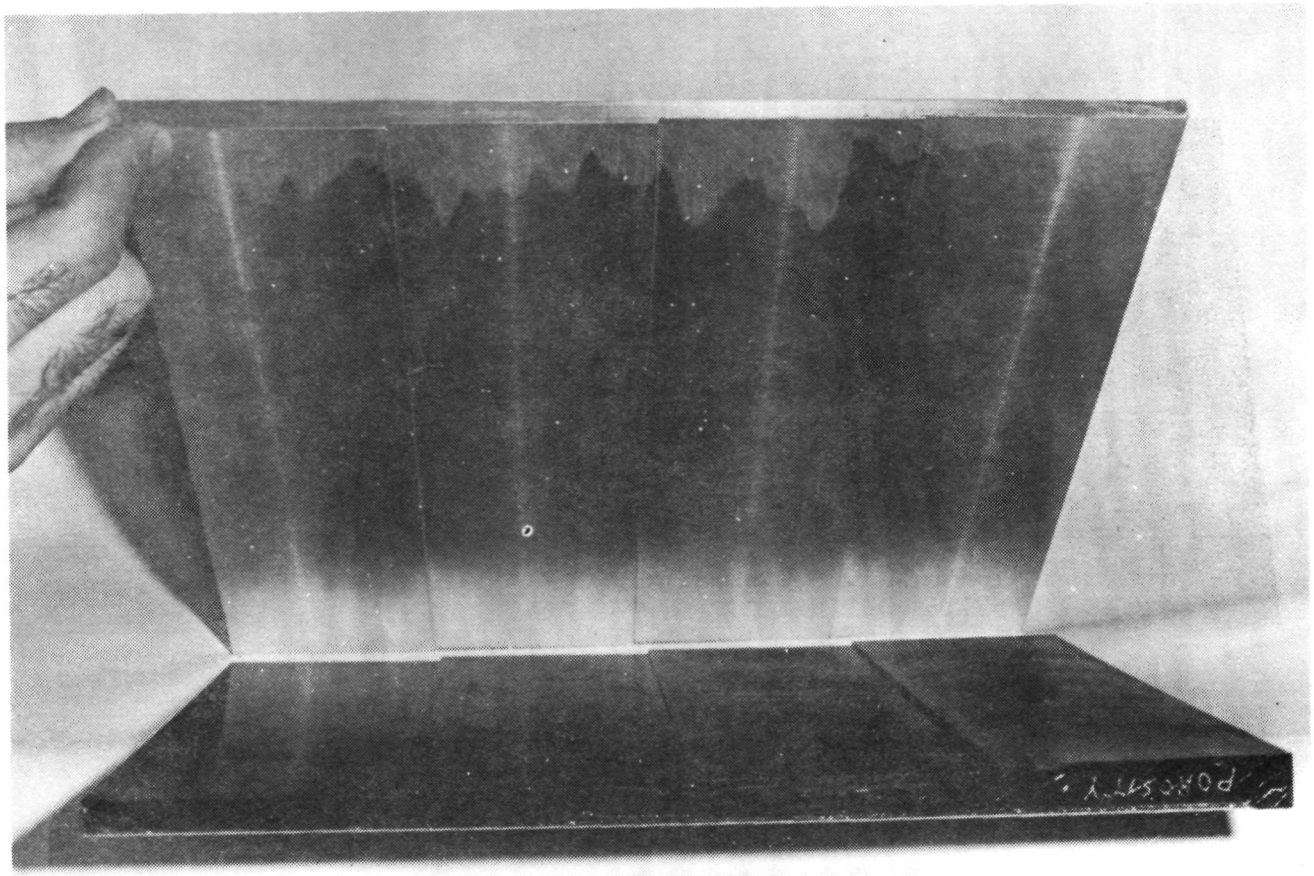

FIGURE 3. USE OF CAUL PLATE TO MOLD PANEL THICKNESS STEPS.

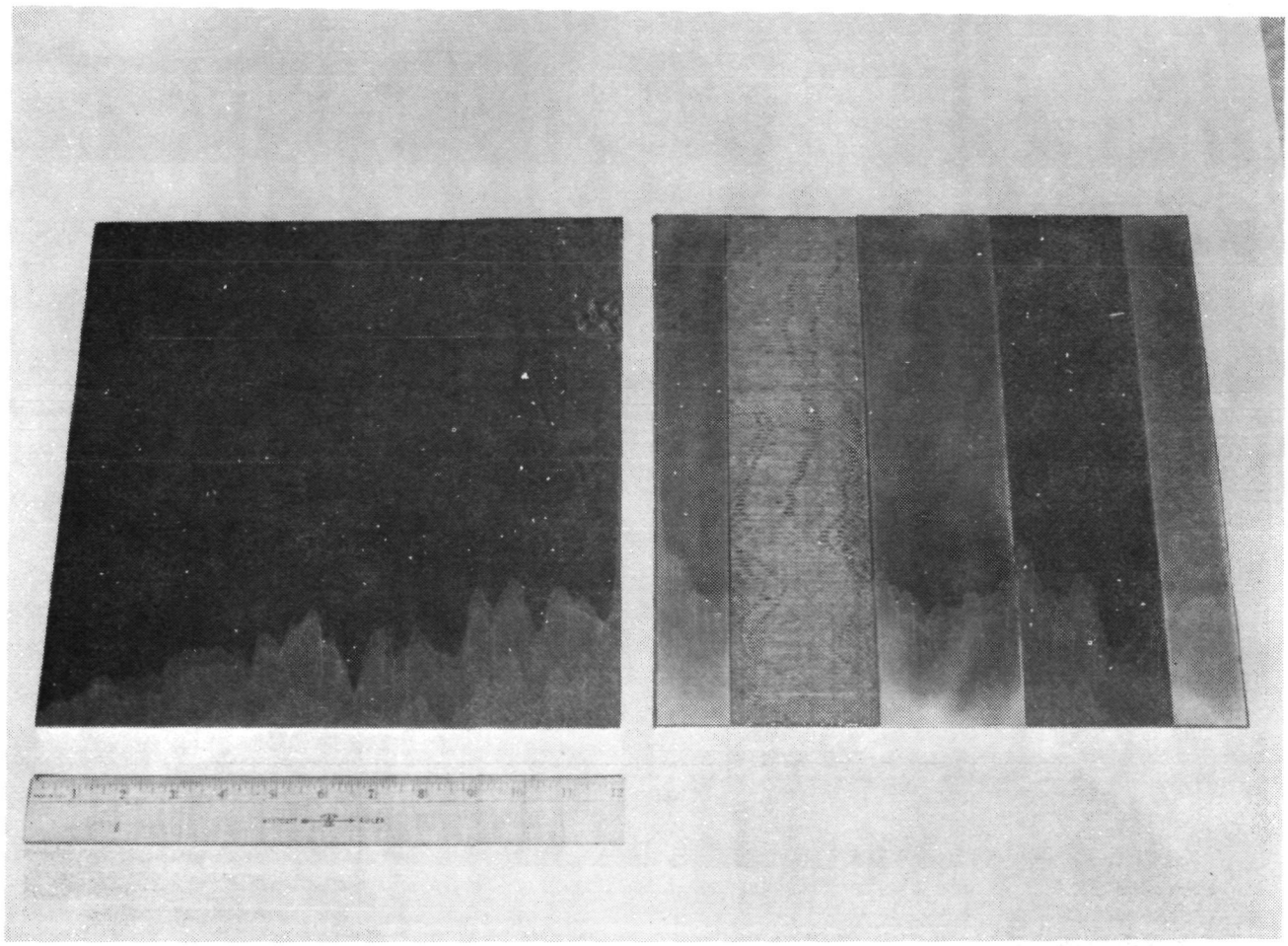

FIGURE 4. FRONT AND BACK FACES OF A TYPICAL PANEL.

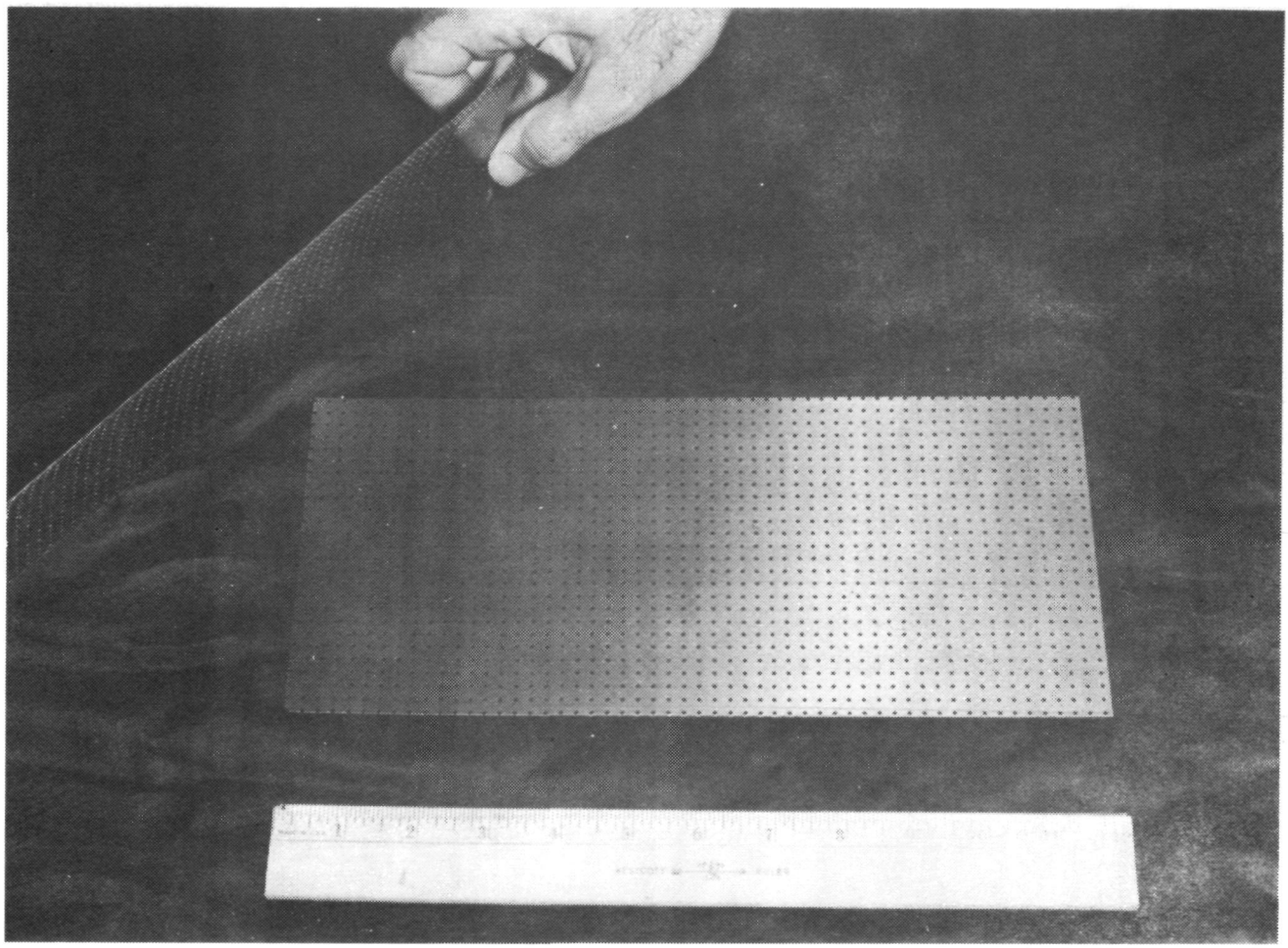

FIGURE 5. PERFORATED TITANIUM SHIMS USED IN TWO OF THE PANELS.

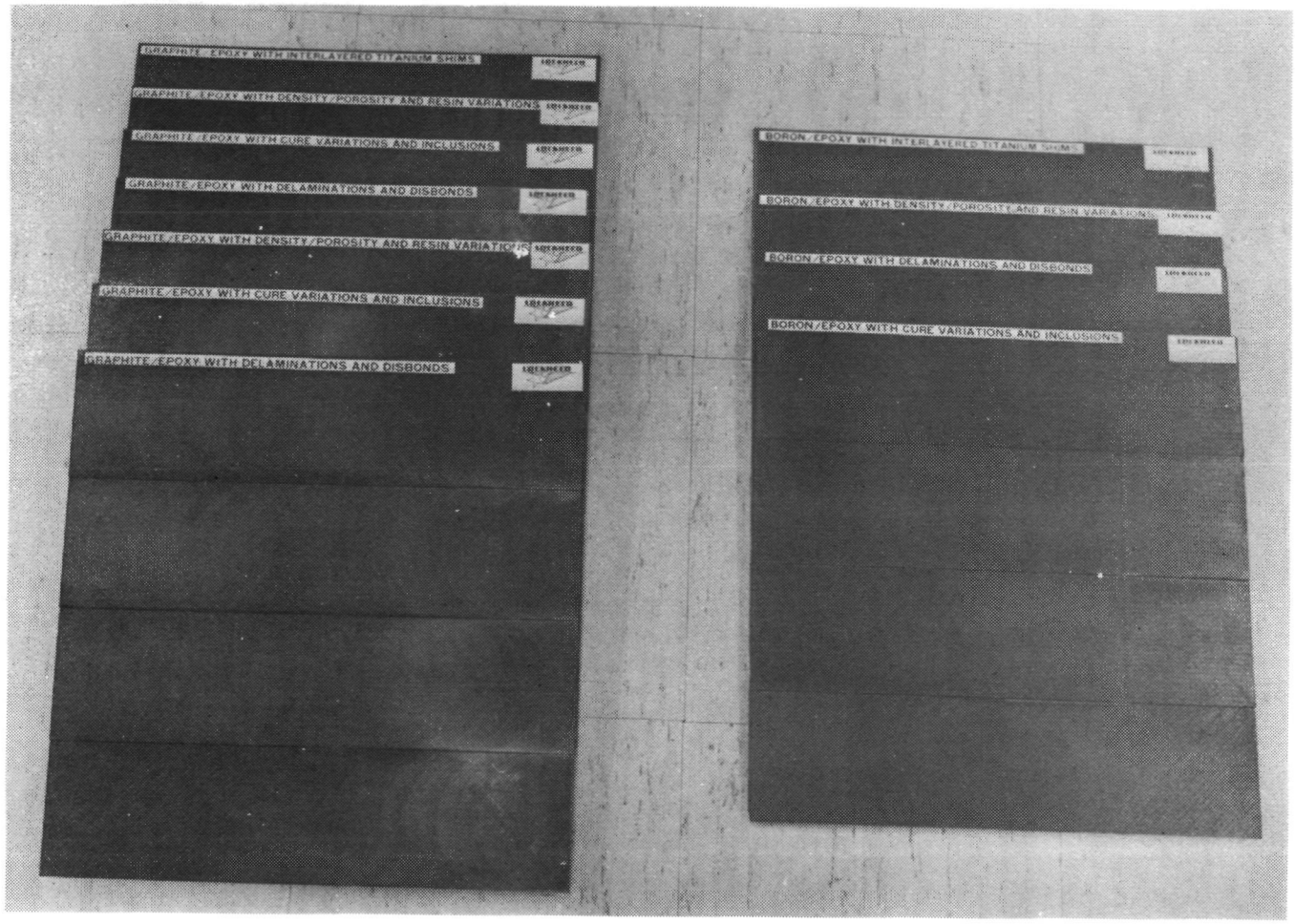

FIGURE 6. FINISHED PANELS READY FOR SHIPMENT.

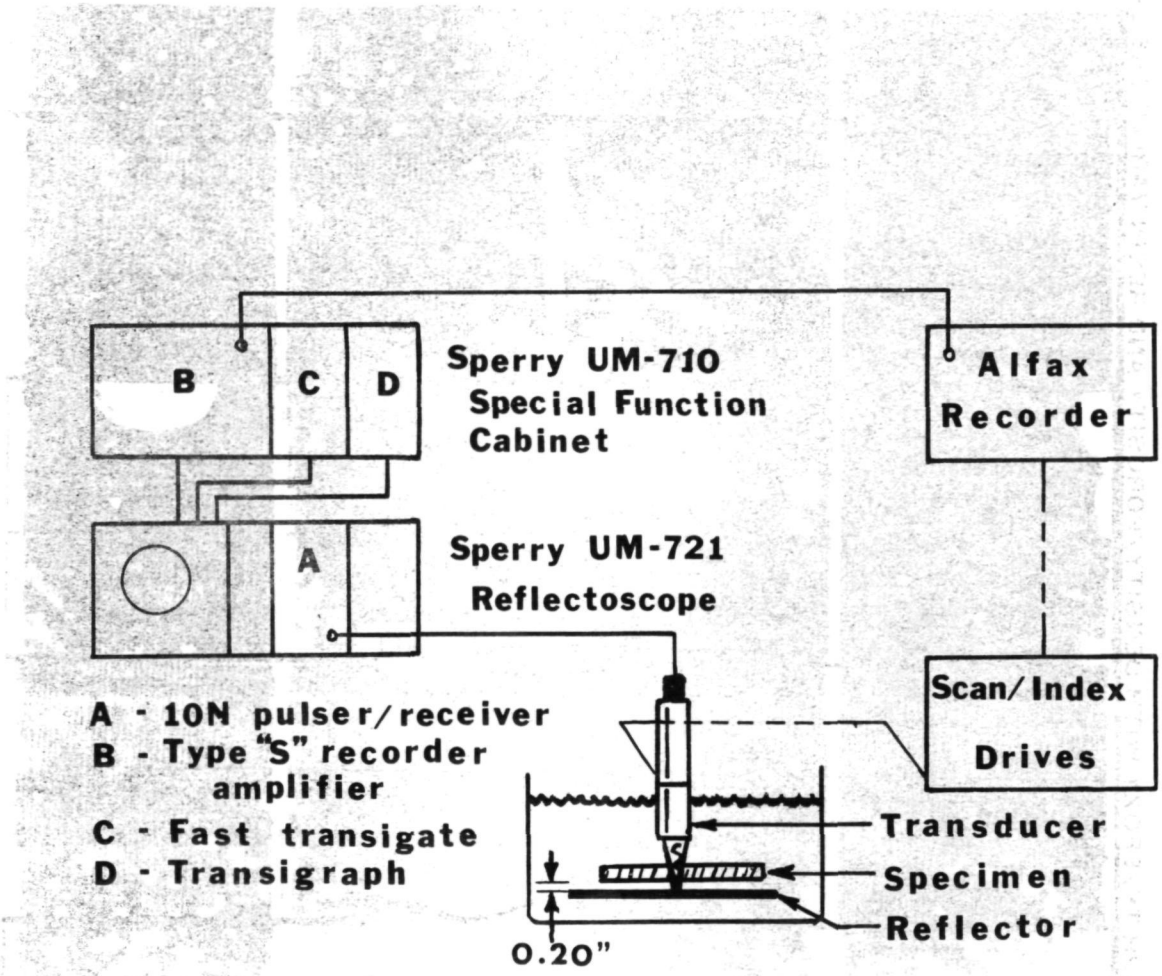

FIGURE 7. BLOCK DIAGRAM OF ULTRASONIC C-SCAN INSPECTION SYSTEM.

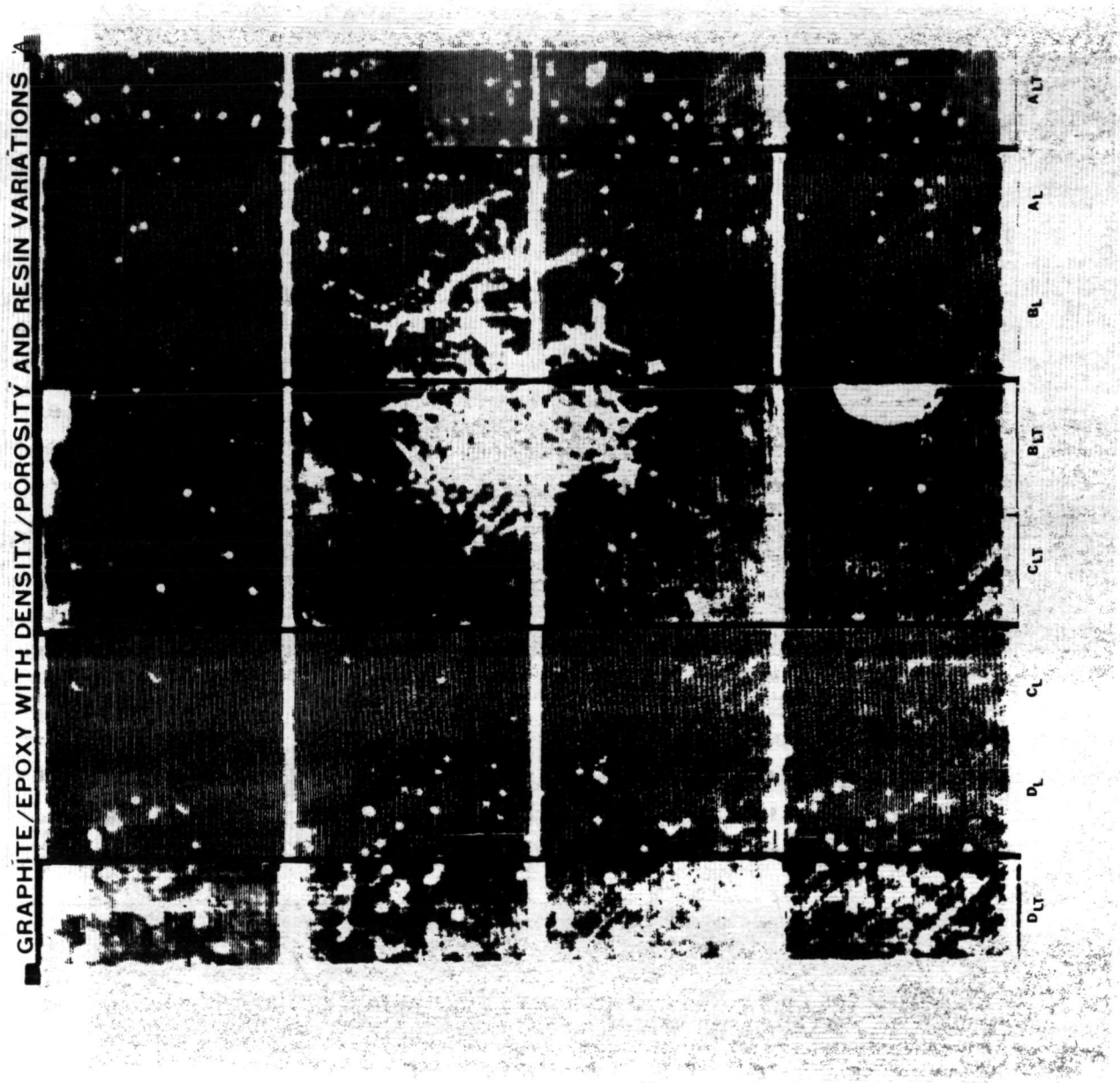

FIGURE 8. ULTRASONIC C-SCAN OF GRAPHITE/EPOXY DENSITY/POROSITY & RESIN VARIATION PANEL, THICKNESS A.

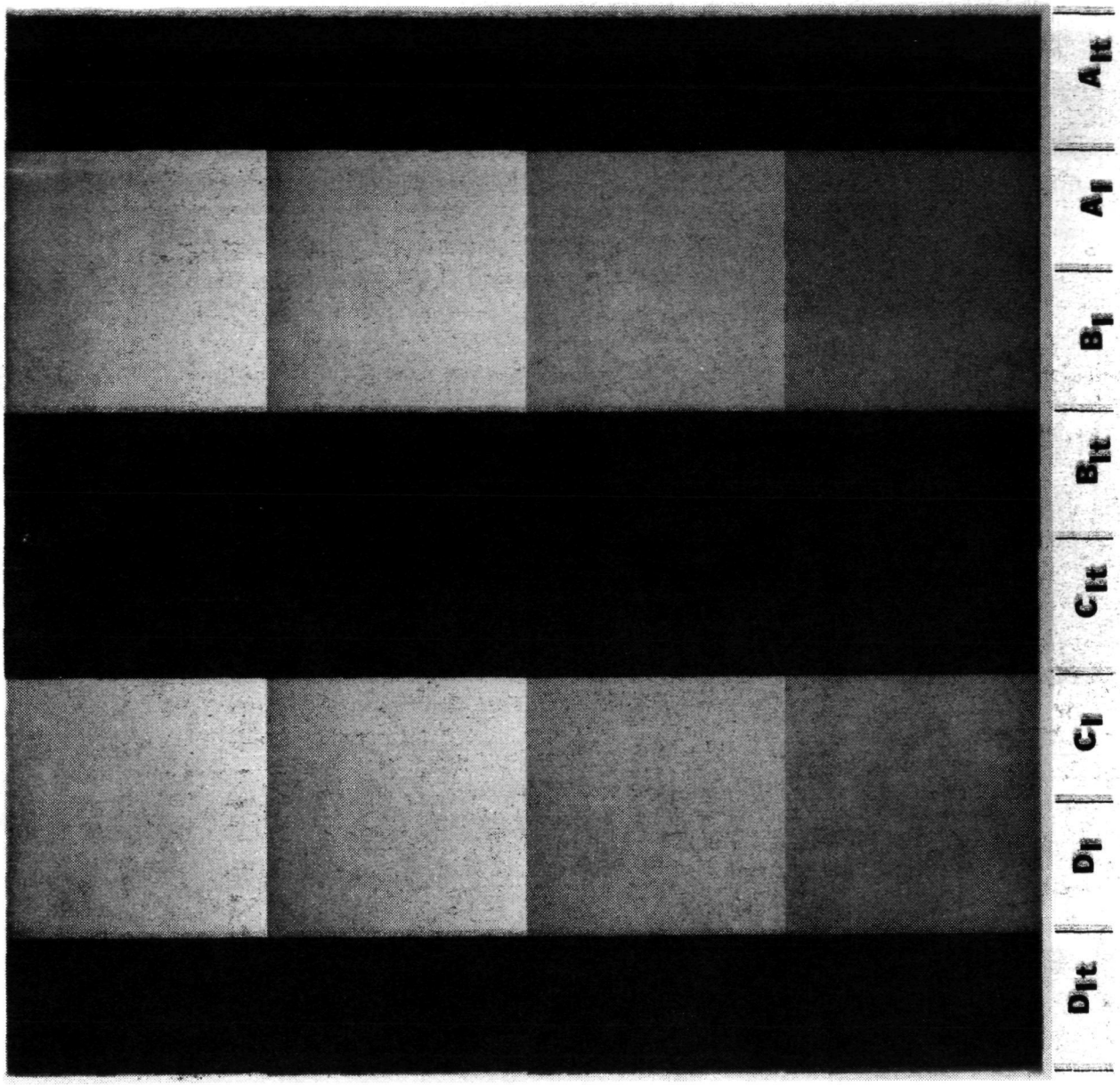

FIGURE 9. RADIOGRAPH C-SCAN OF GRAPHITE/EPOXY DENSITY/ POROSITY & RESIN VARIATION PANEL, THICKNESS A. PLAIN AREAS. EXPOSURE 45 SECONDS.

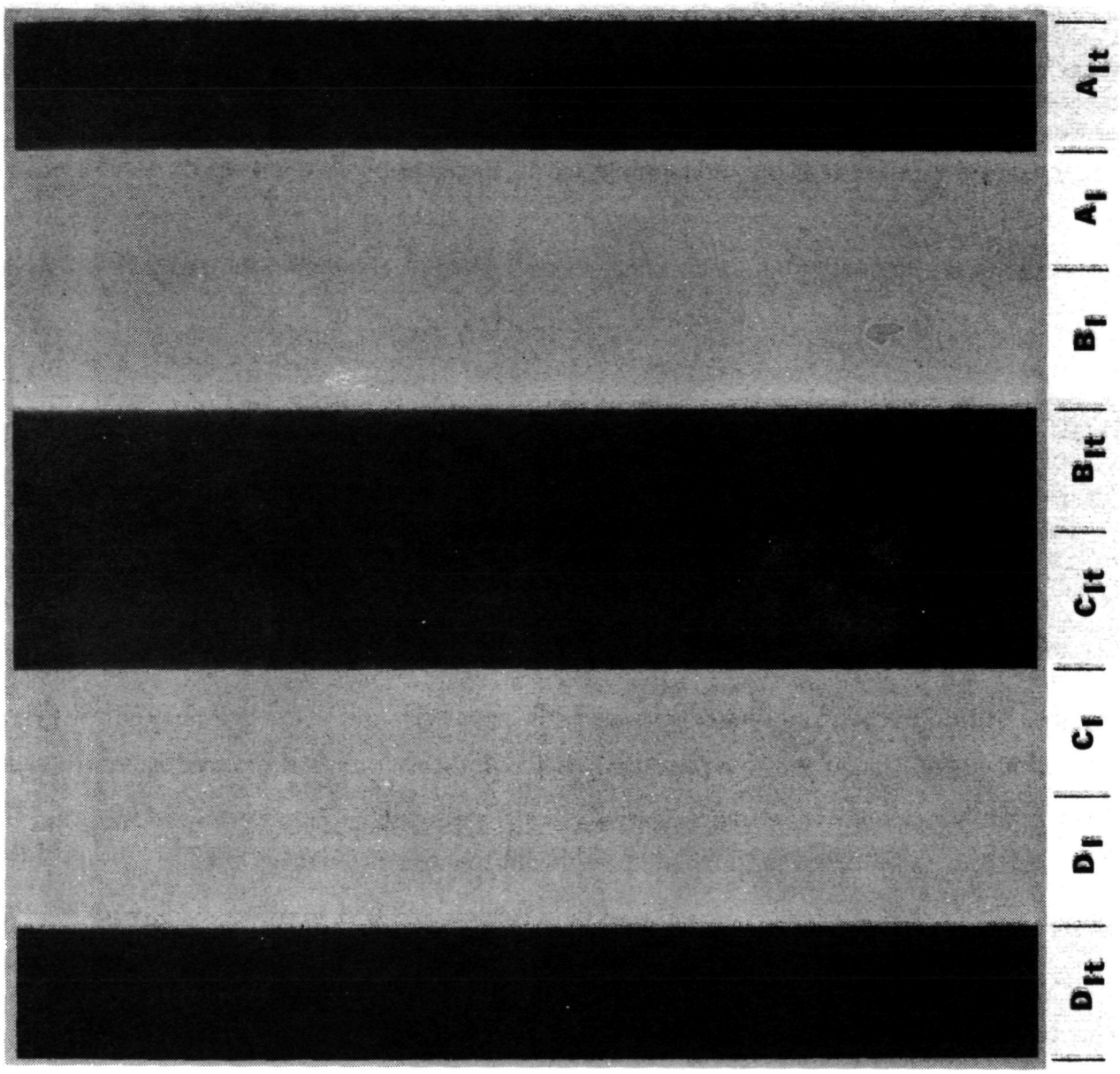

FIGURE 10. RADIOGRAPH OF GRAPHITE/EPOXY DENSITY/POROSITY & RESIN VARIATION PANEL, THICKNESS A, SUBSTRATE AREAS. EXPOSURE 2 MINUTES.

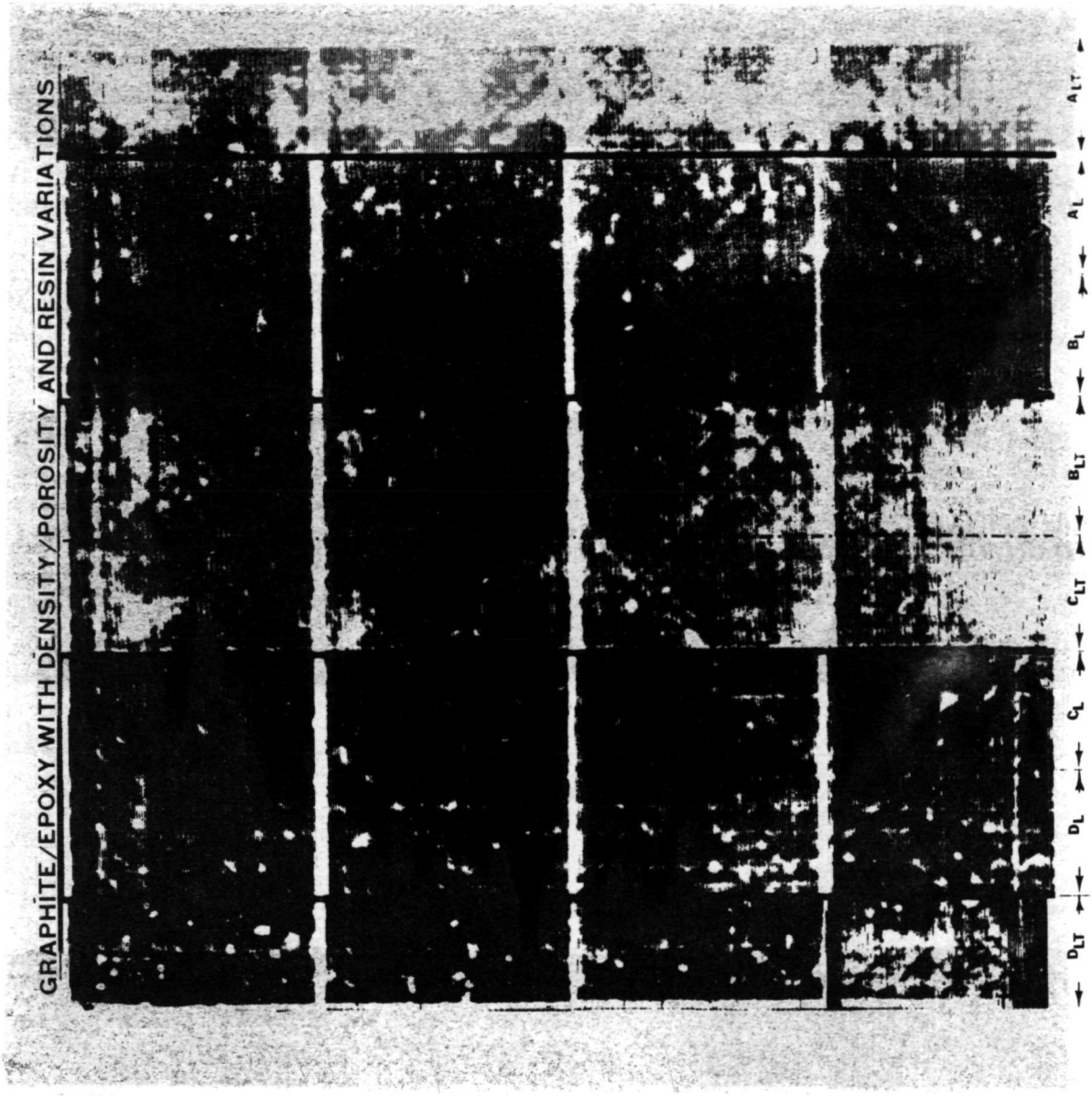

FIGURE 11. ULTRASONIC C-SCAN OF GRAPHITE/EPOXY DENSITY/ POROSITY & RESIN VARIATION PANEL, THICKNESS B.

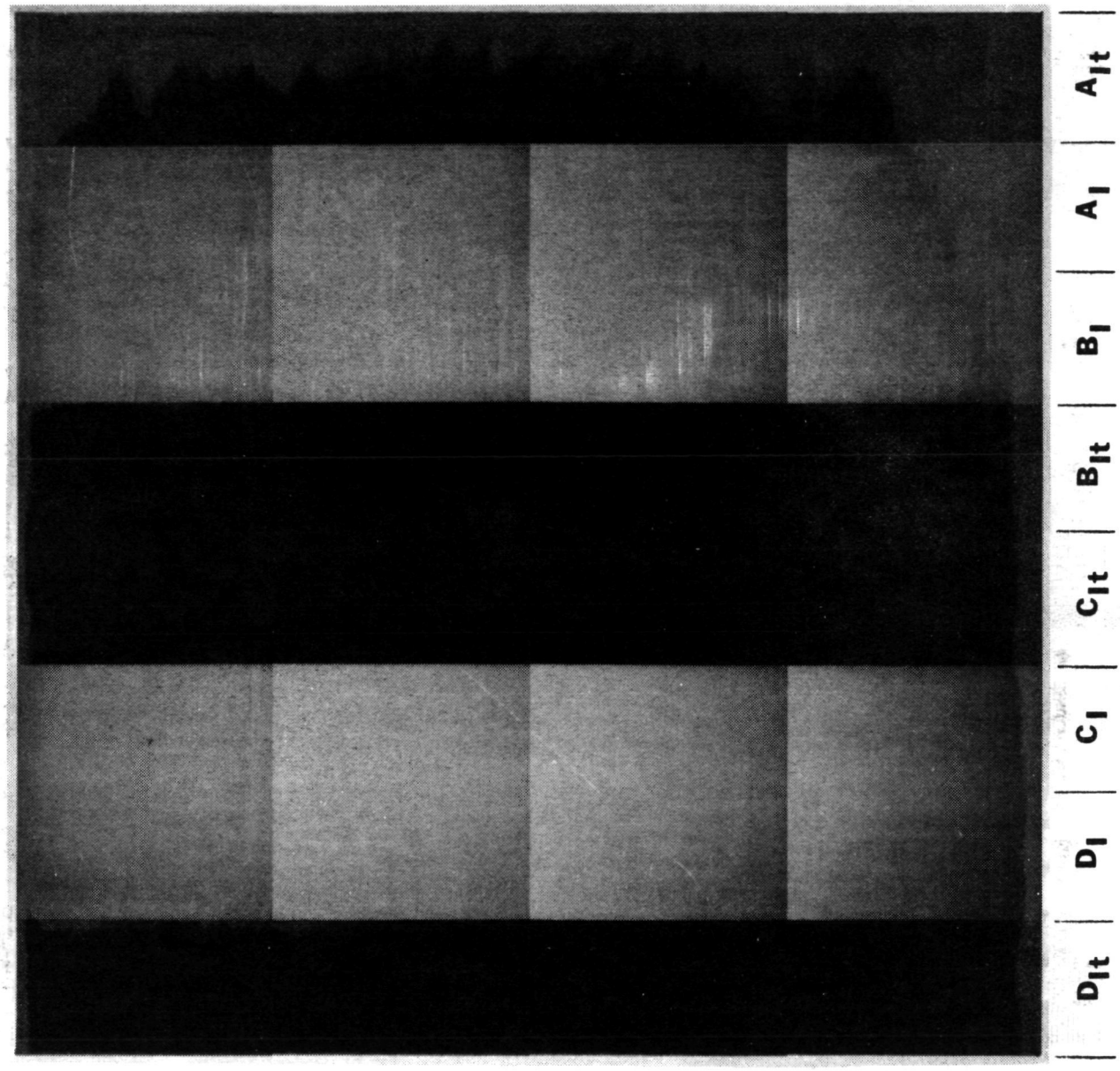

FIGURE 12. RADIOGRAPH OF GRAPHITE/EPOXY DENSITY/POROSITY & RESIN VARIATION PANEL, THICKNESS B, PLAIN AREAS. EXPOSURE 60 SECONDS.

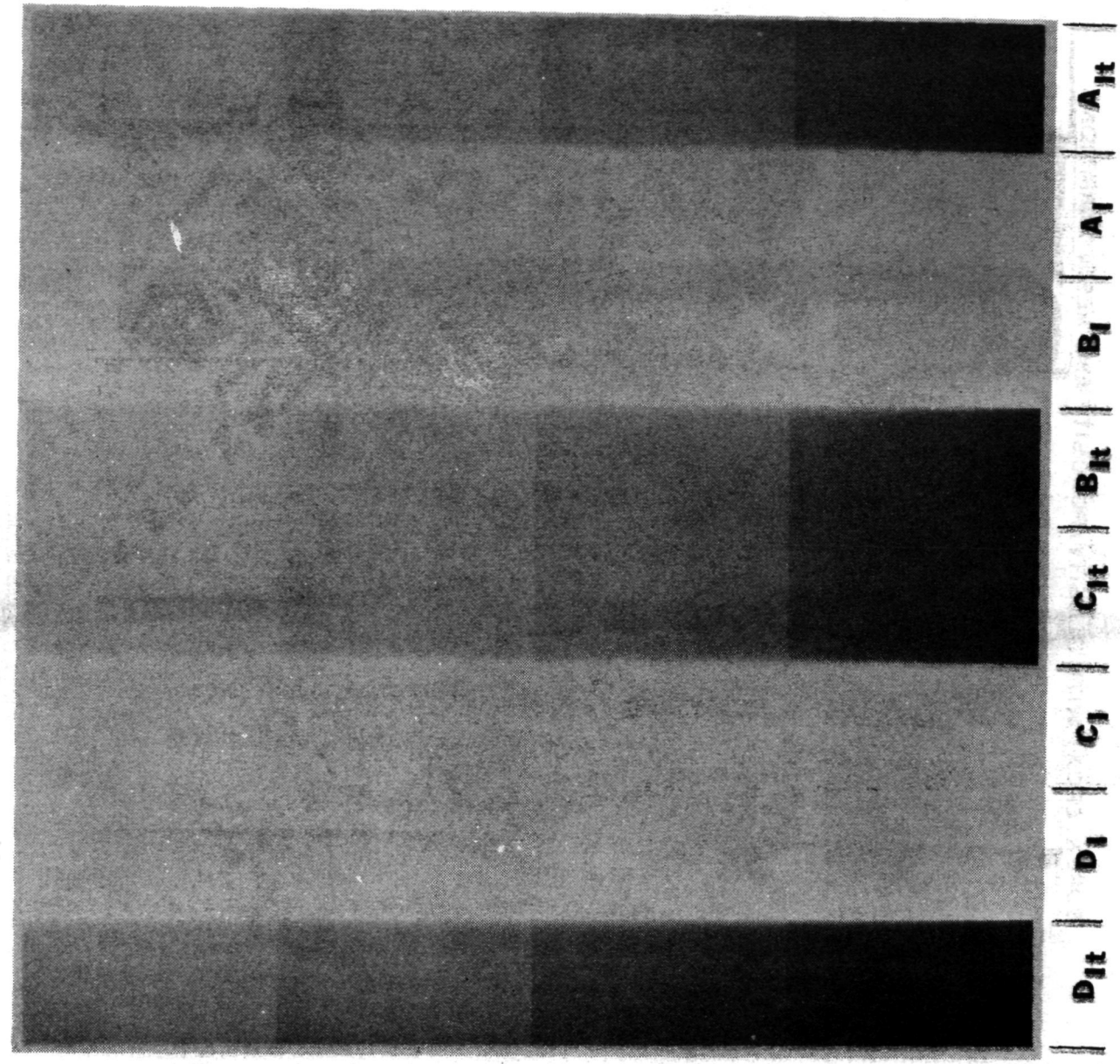

FIGURE 13. RADIOGRAPH OF GRAPHITE/EPOXY DENSITY/POROSITY & RESIN VARIATION PANEL, THICKNESS B, SUBSTRATE AREAS. EXPOSURE 2 MINUTES.

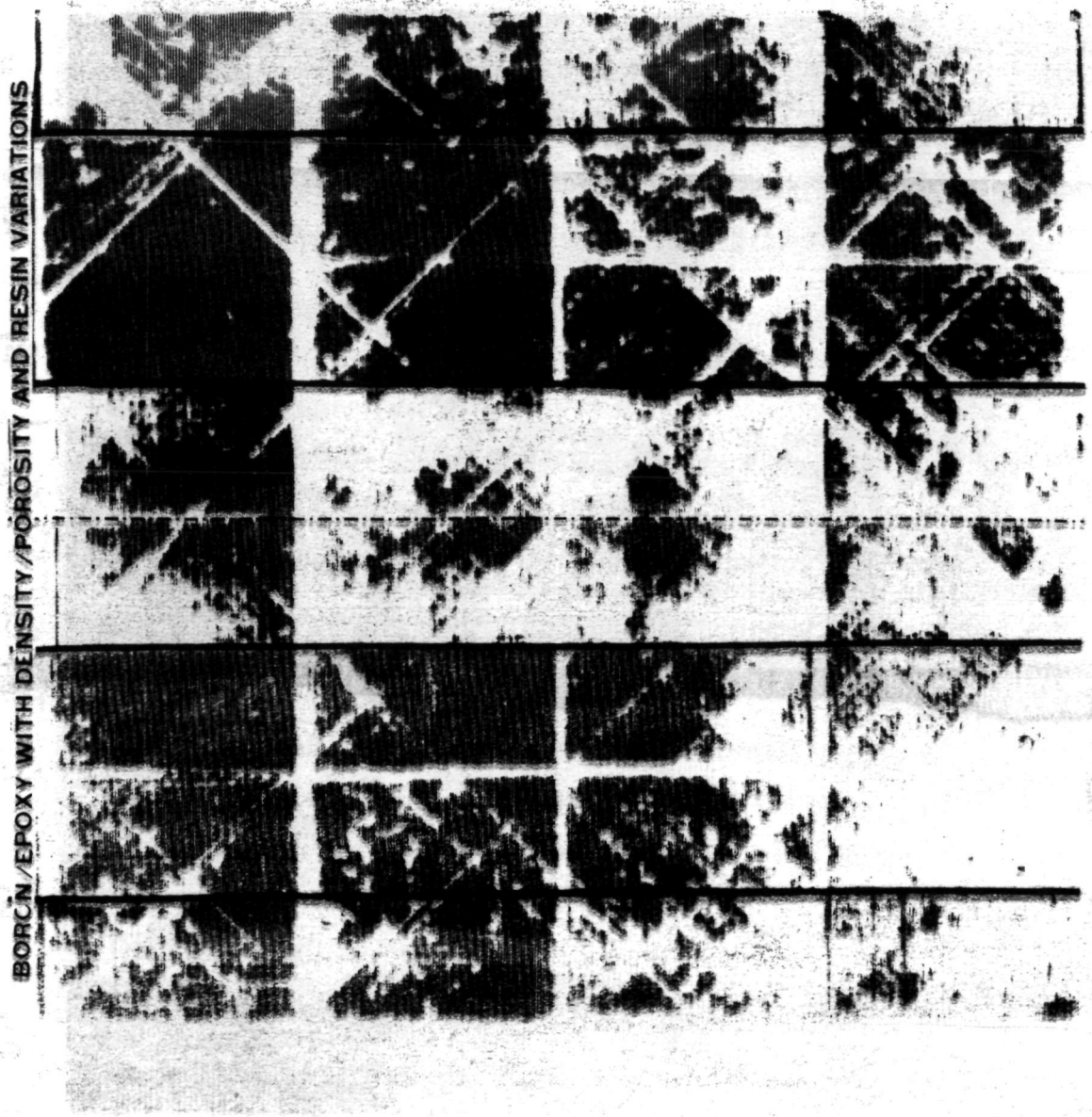

FIGURE 14. ULTRASONIC C-SCAN OF BORON/EPOXY DENSITY/ POROSITY & RESIN VARIATION PANEL.

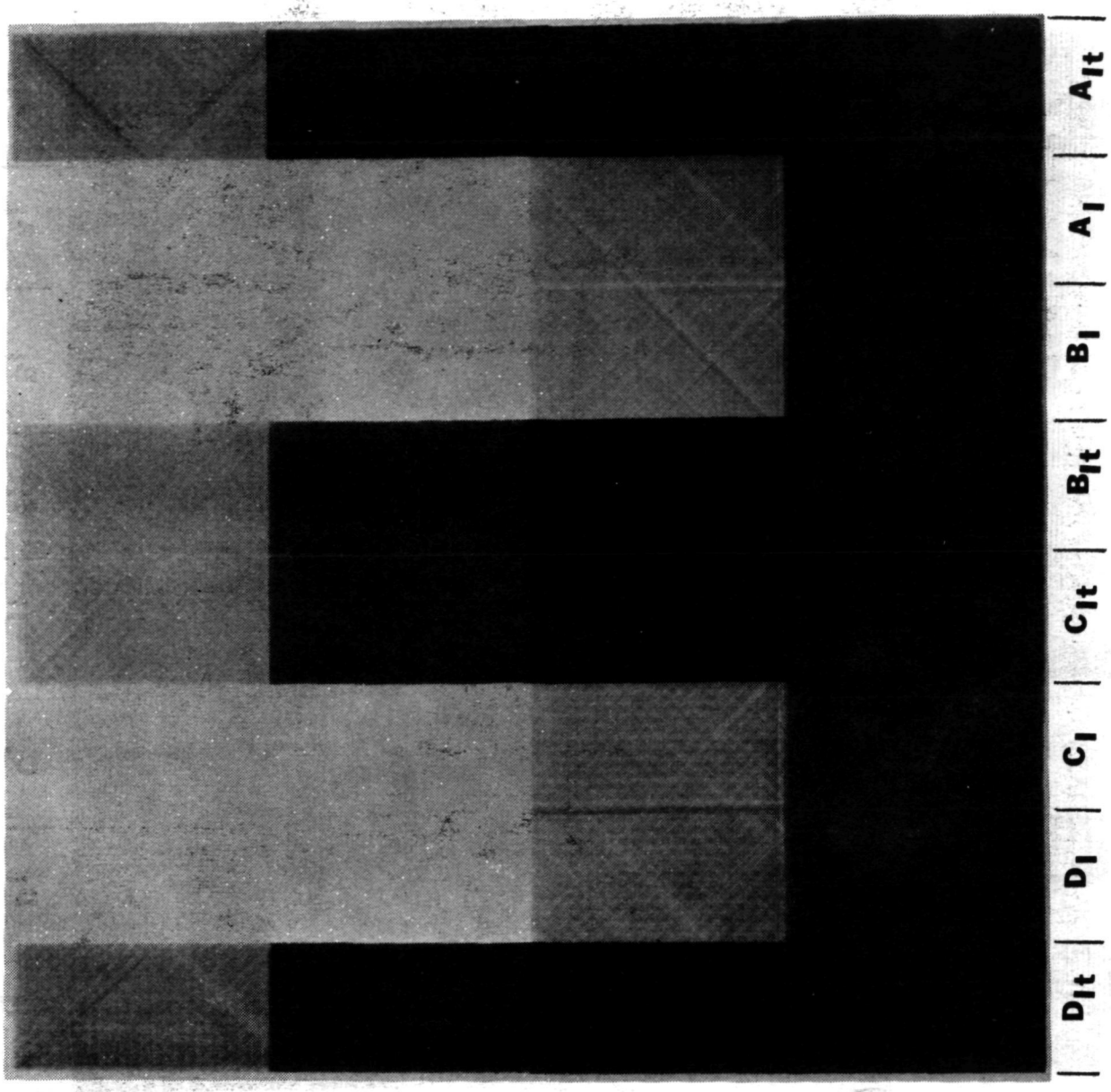

FIGURE 15. RADIOGRAPH OF BORON/EPOXY DENSITY/POROSITY & RESIN VARIATION PANEL, PLAIN AREAS. EXPOSURE 2.5 MINUTES.

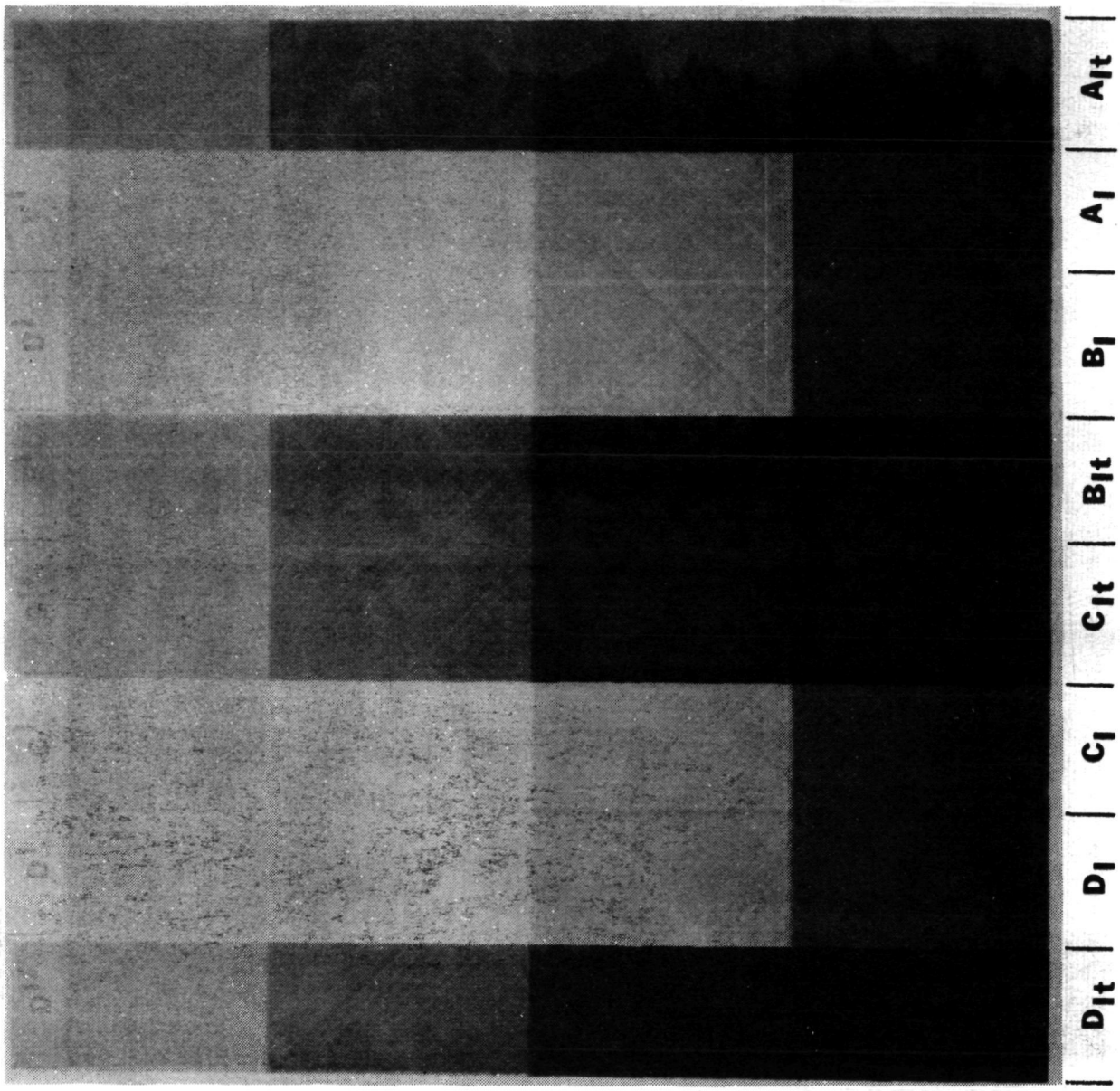

FIGURE 16. RADIOGRAPH OF BORON/EPOXY DENSITY/POROSITY & RESIN VARIATION PANEL, SUBSTRATE AREAS. EXPOSURE 5 MINUTES.

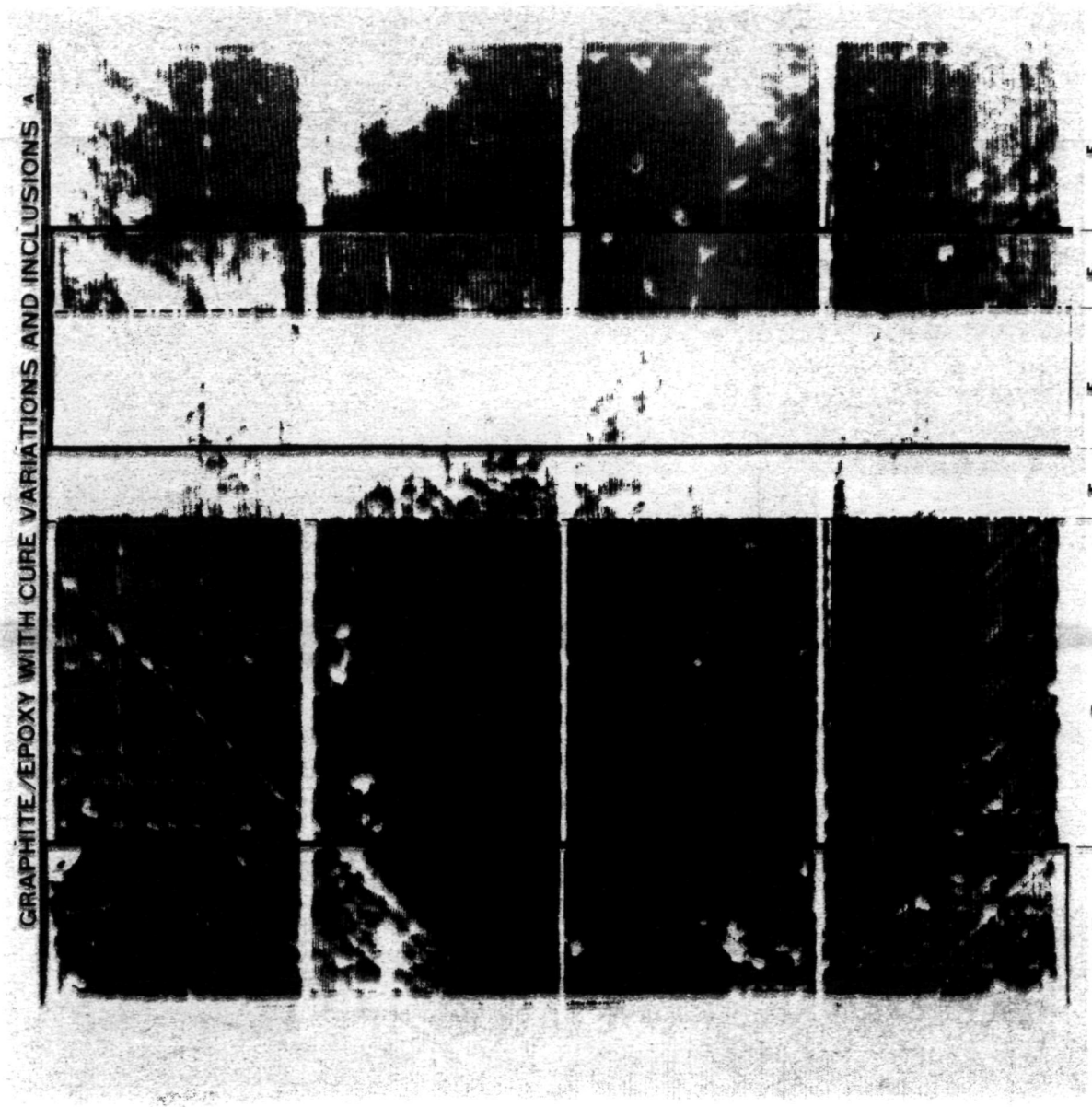

FIGURE 17. ULTRASONIC C-SCAN OF GRAPHITE/EPOXY CURE VARIATIONS AND INCLUSIONS PANEL, THICKNESS A.

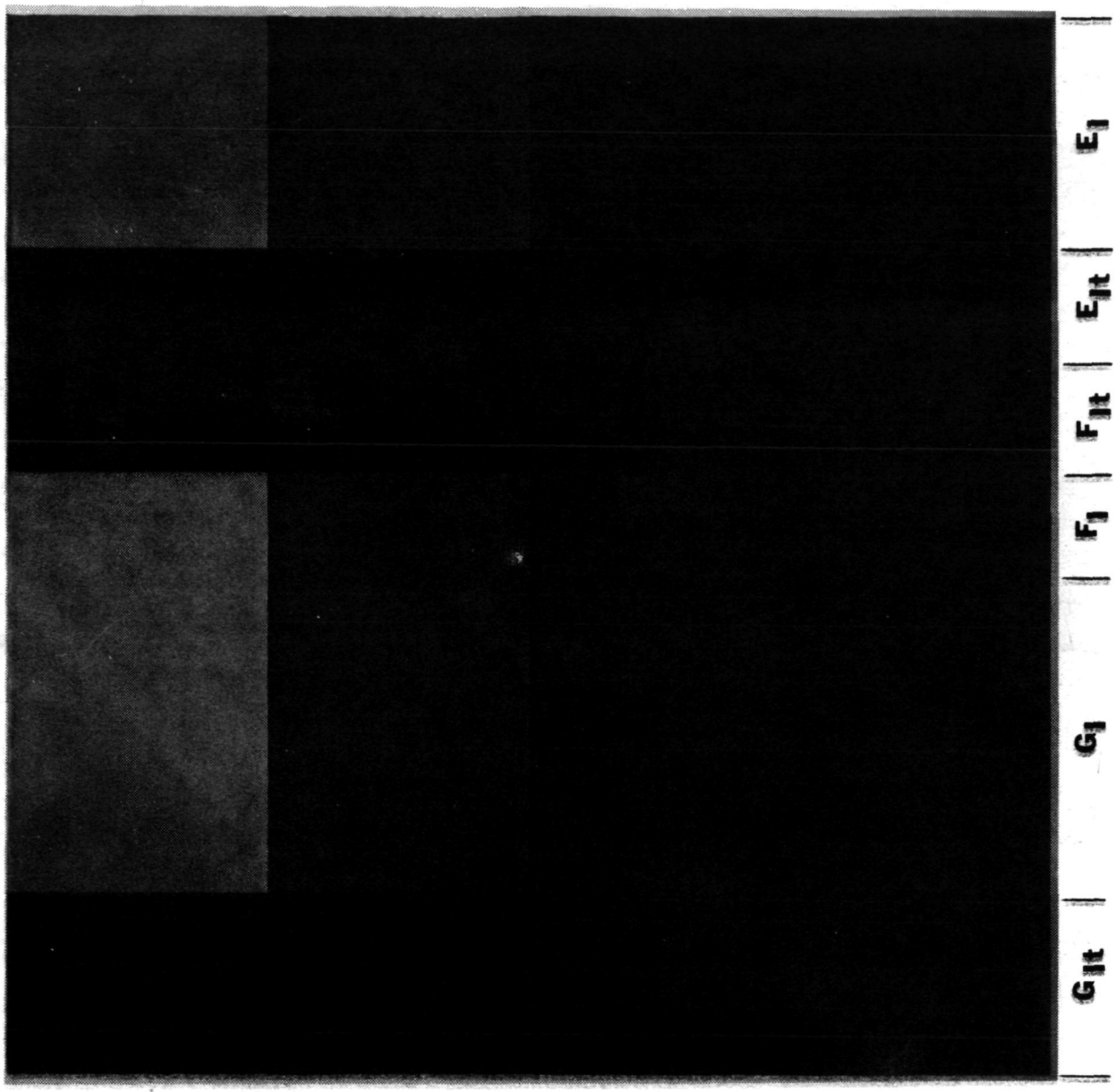

FIGURE 18. RADIOGRAPH OF GRAPHITE/EPOXY CURE VARIATIONS AND INCLUSIONS PANEL, THICKNESS A, PLAIN AREAS, EXPOSURE 30 SECONDS.

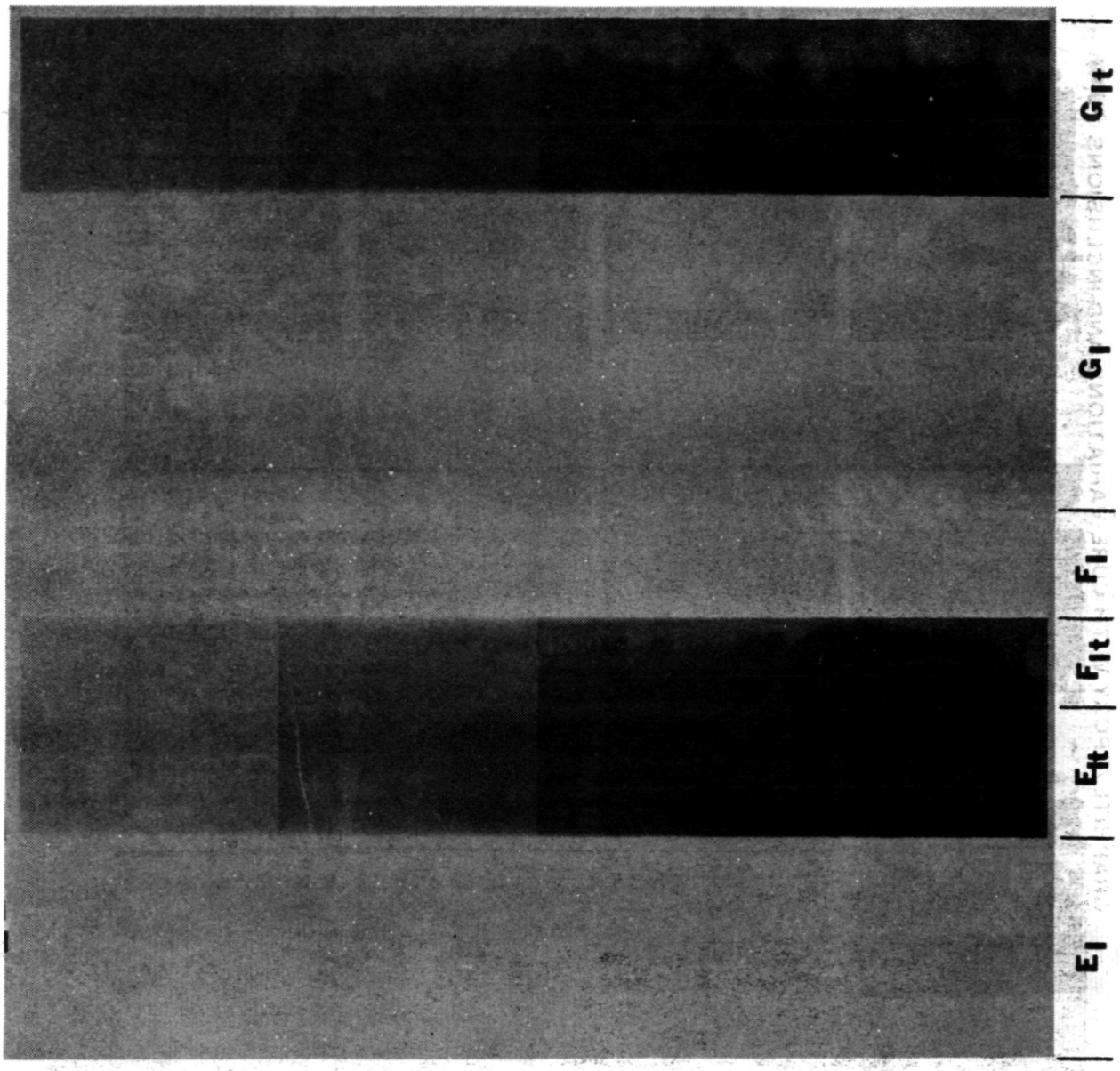

FIGURE 19. RADIOGRAPH OF GRAPHITE/EPOXY CURE VARIATIONS AND INCLUSIONS PANEL, THICKNESS A, SUBSTRATE AREAS. EXPOSURE 3 MINUTES.

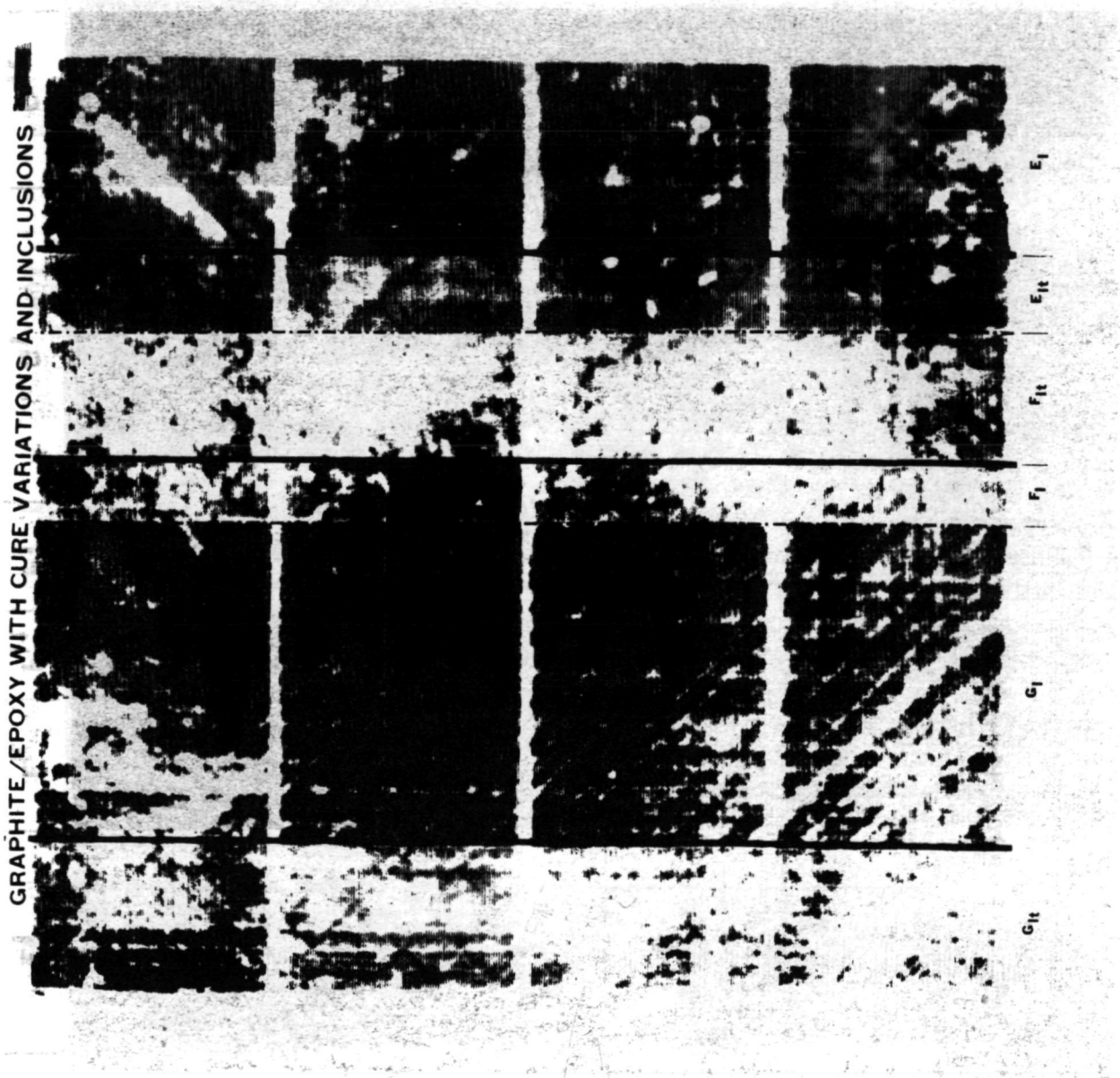

FIGURE 20. ULTRASONIC C-SCAN OF GRAPHITE/EPOXY CURE VARIATIONS AND INCLUSIONS PANEL, THICKNESS B.

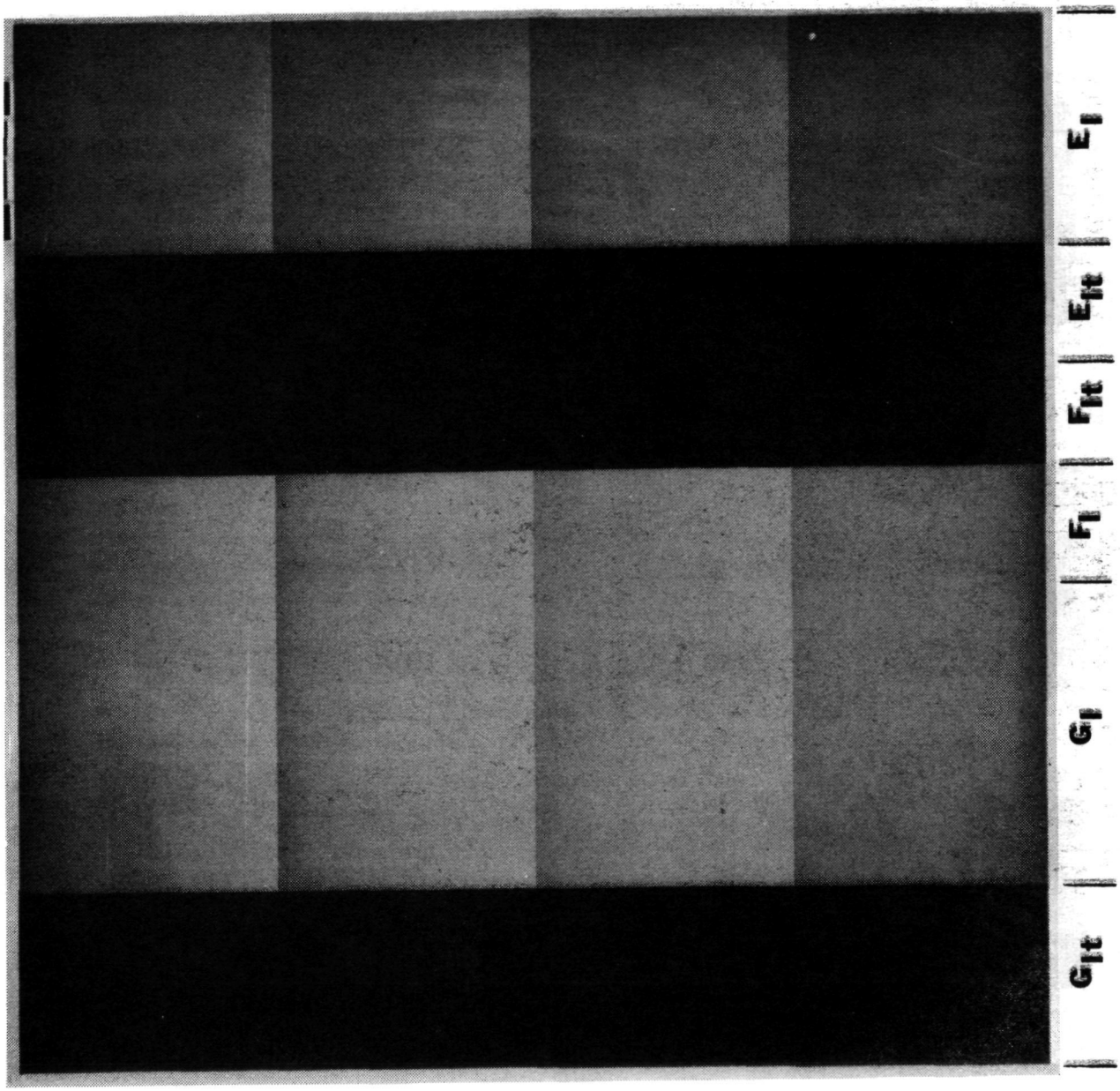

FIGURE 21. RADIOGRAPH OF GRAPHITE/EPOXY CURE VARIATIONS AND INCLUSIONS PANEL, THICKNESS B, PLAIN AREAS. EXPOSURE 60 SECONDS.

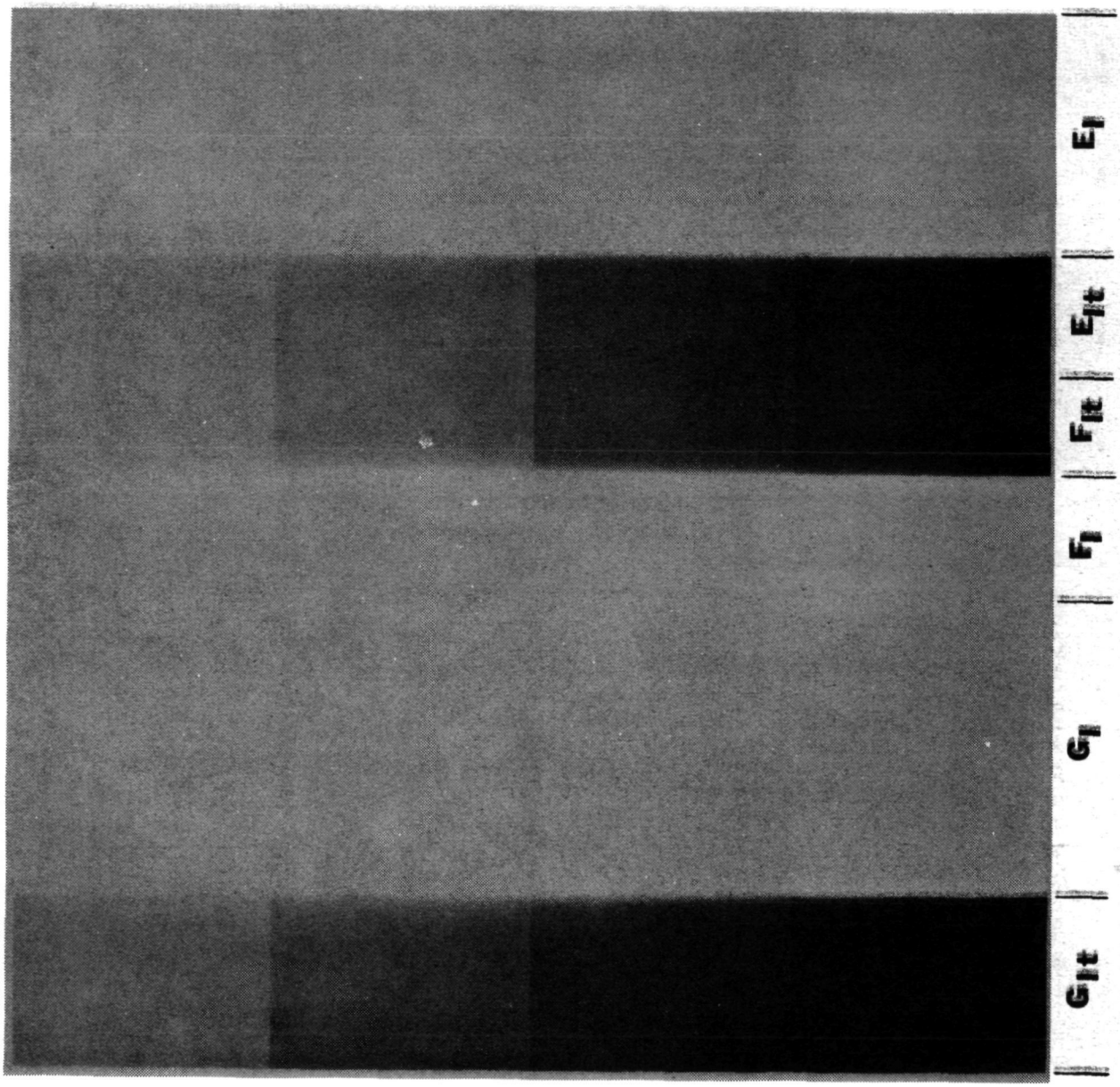

FIGURE 22. RADIOGRAPH OF GRAPHITE/EPOXY CURE VARIATIONS AND INCLUSIONS PANEL, THICKNESS B, SUBSTRATE AREAS. EXPOSURE 3 MINUTES.

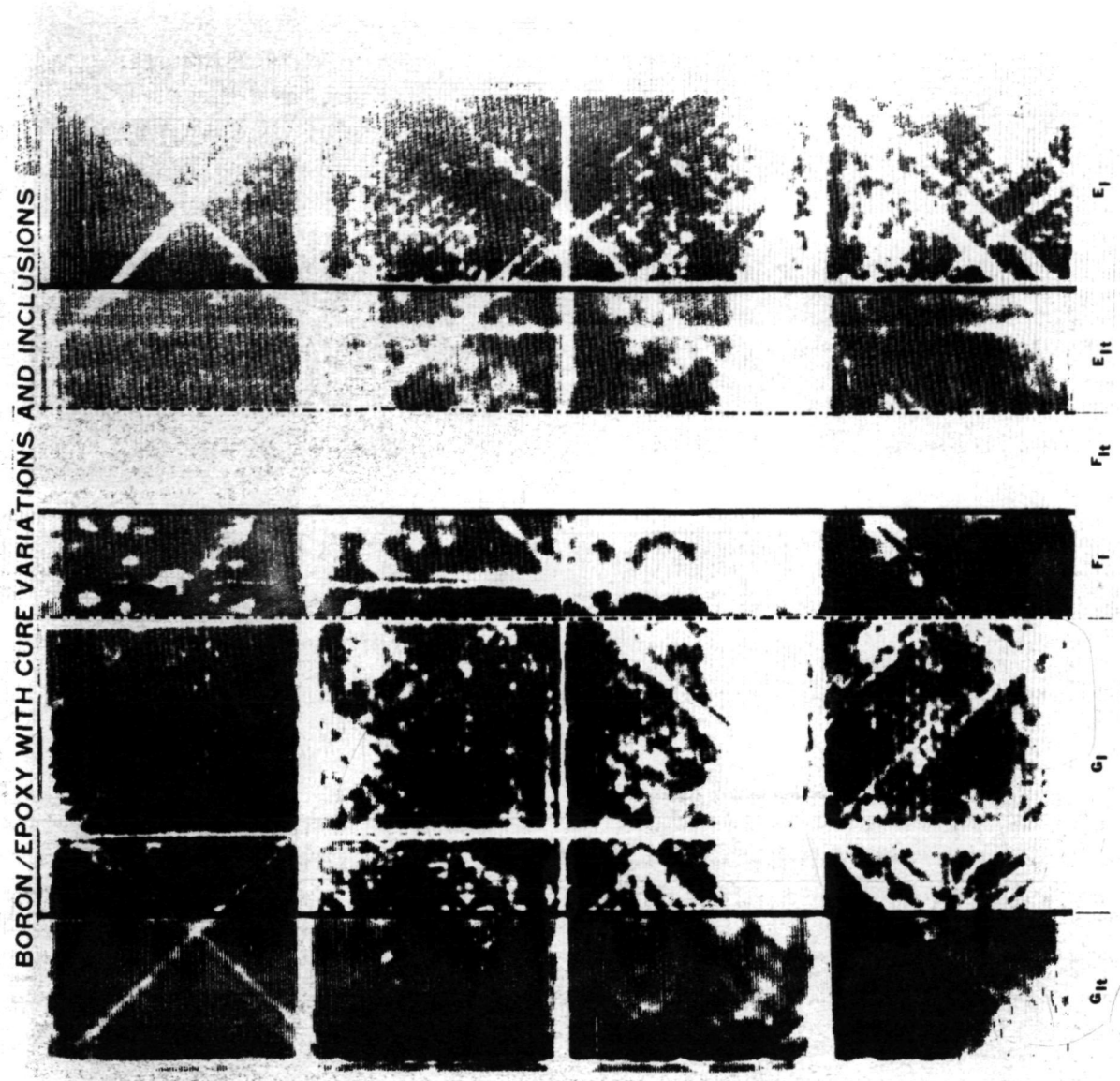

FIGURE 23. ULTRASONIC C-SCAN OF BORON/EPOXY CURE VARIATIONS AND INCLUSIONS PANEL.

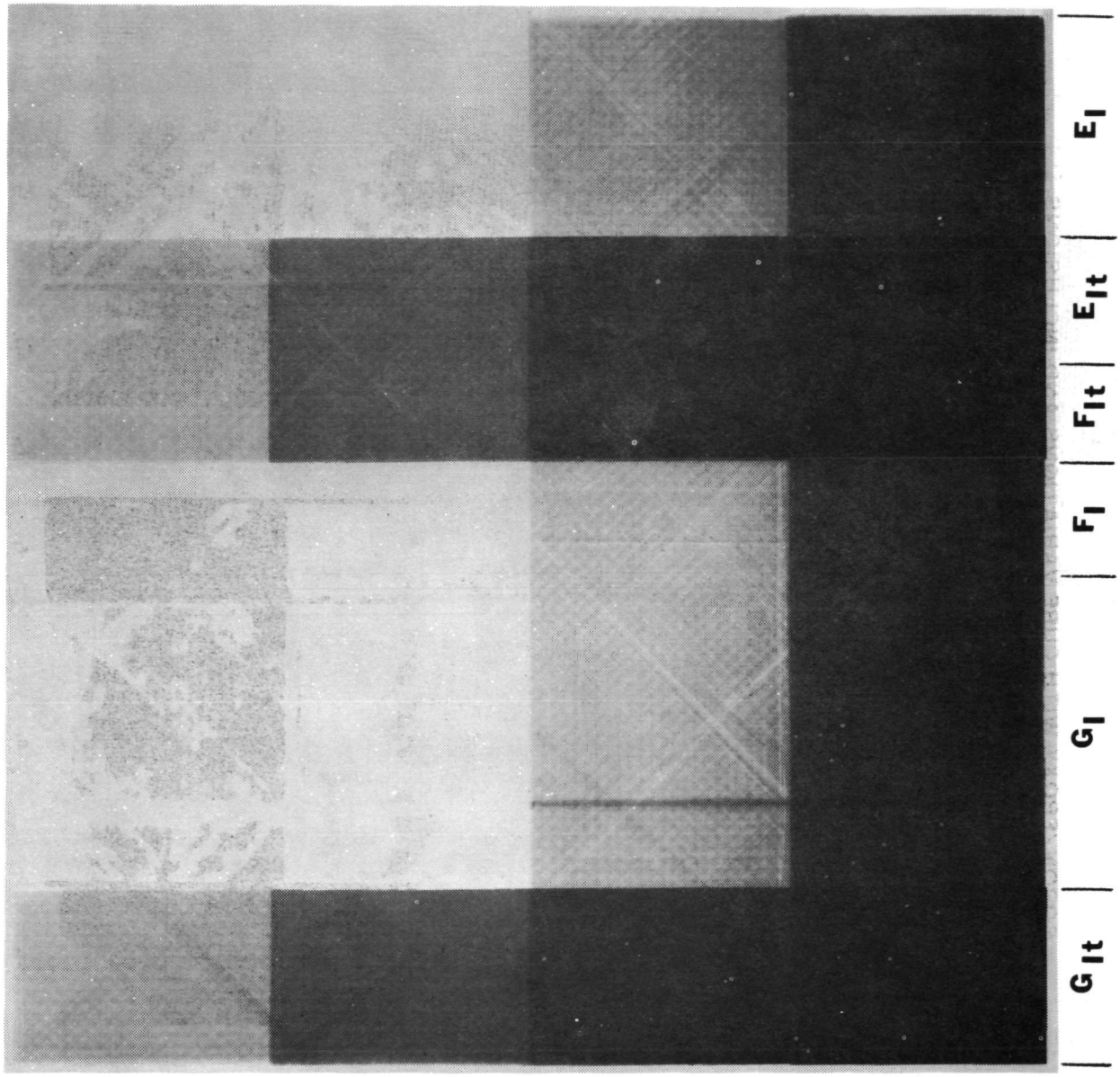

FIGURE 24. RADIOGRAPH OF BORON/EPOXY CURE VARIATIONS AND INCLUSIONS PANEL, PLAIN AREAS. EXPOSURE 2.5 MINUTES.

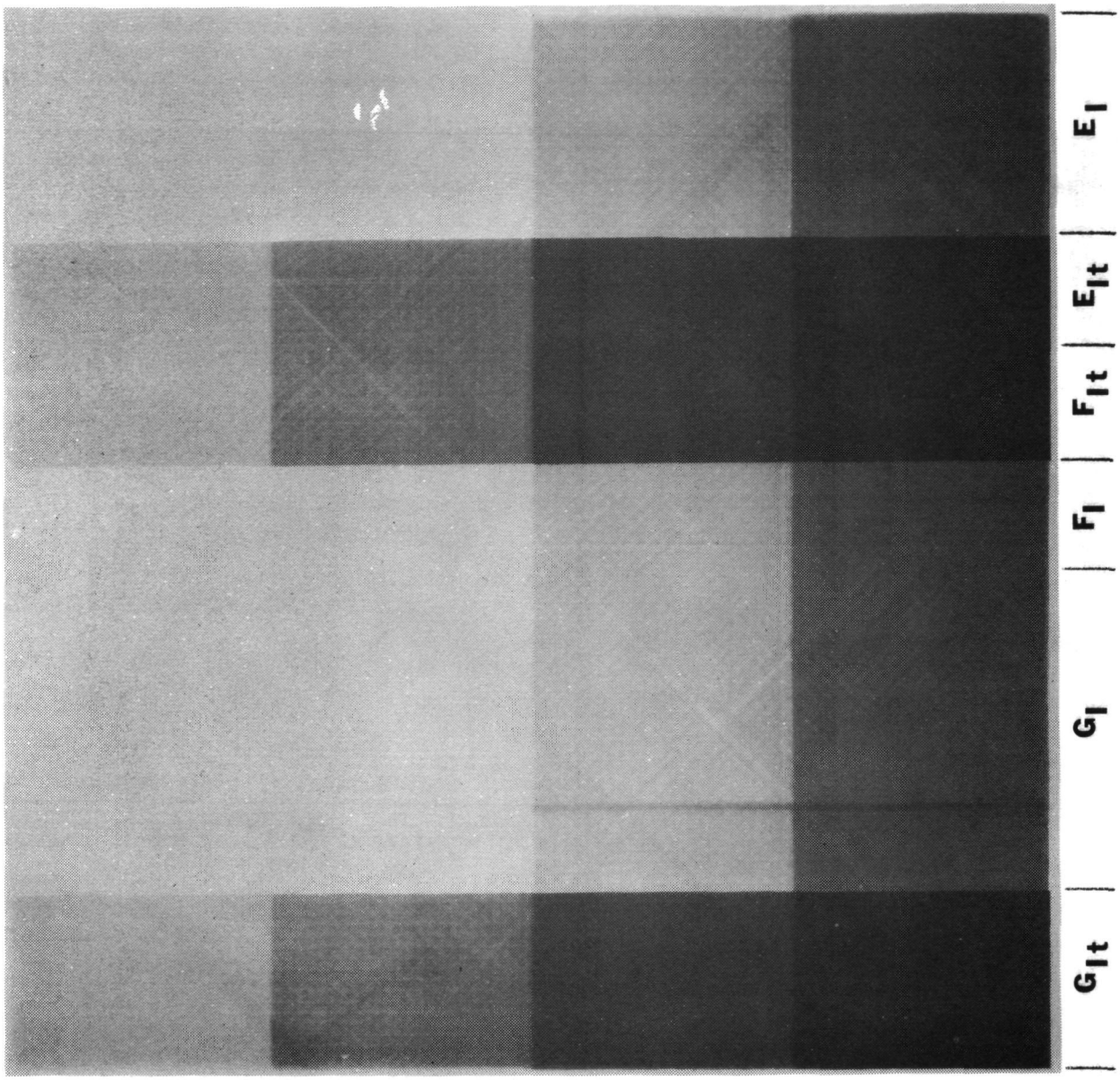

FIGURE 25. RADIOGRAPH OF BORON/EPOXY CURE VARIATIONS AND INCLUSIONS PANEL, SUBSTRATE AREAS. EXPOSURE 5 MINUTES.

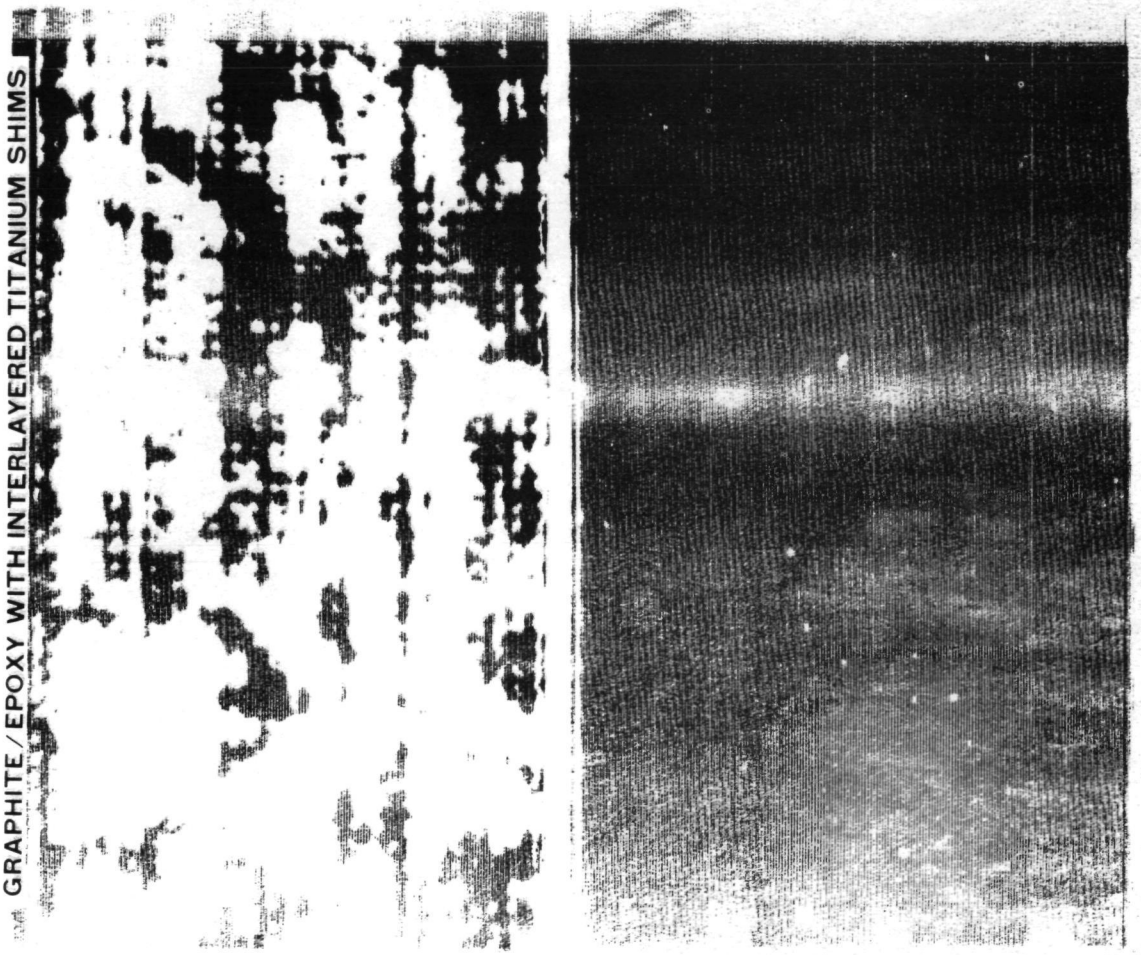

FIGURE 26. ULTRASONIC C-SCAN OF GRAPHITE/EPOXY INTERLAYERED TITANIUM SHIM PANEL.

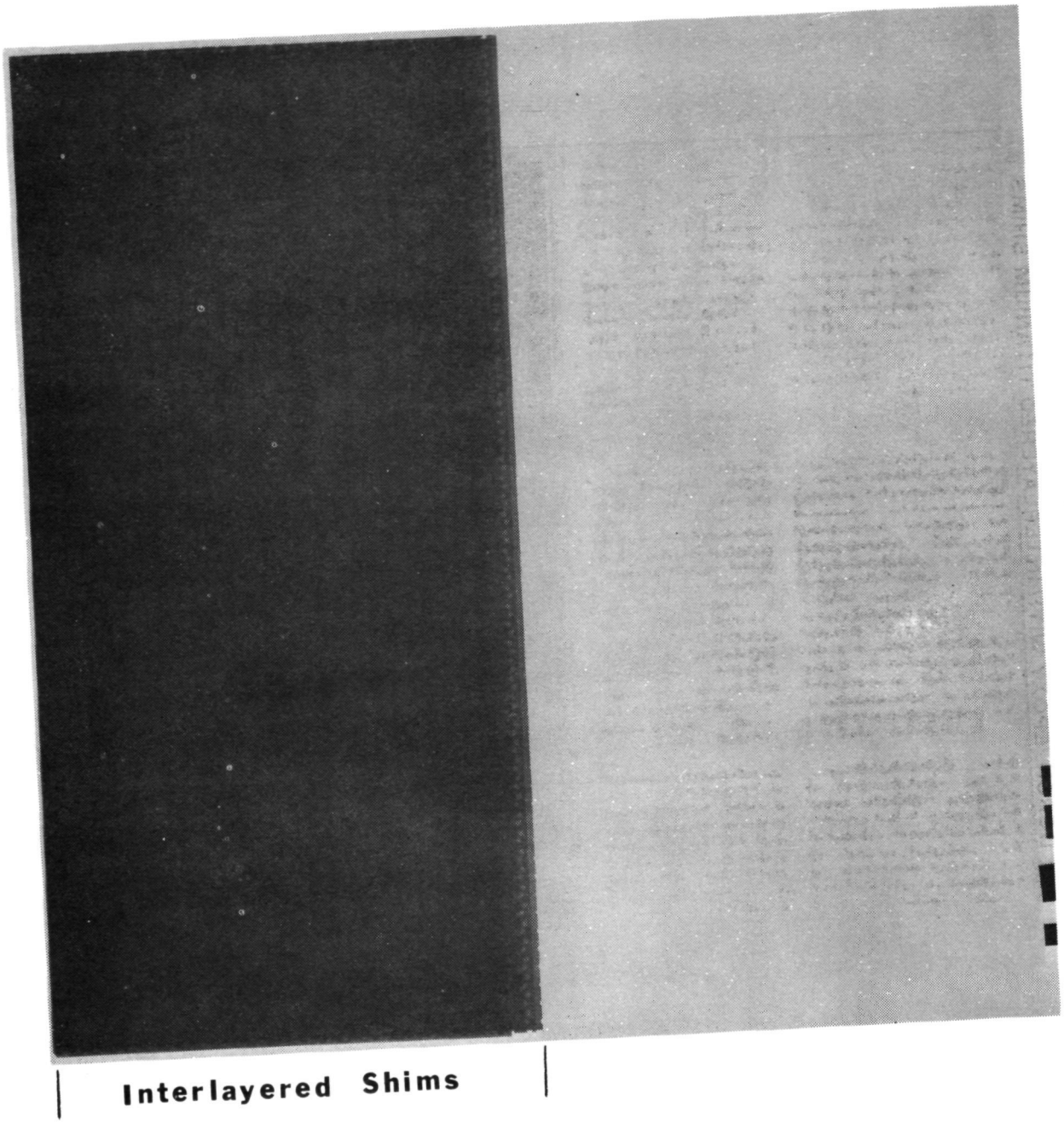

FIGURE 27. RADIOGRAPH OF GRAPHITE/EPOXY INTERLAYERED TITANIUM SHIM PANEL. EXPOSURE 30 SECONDS.

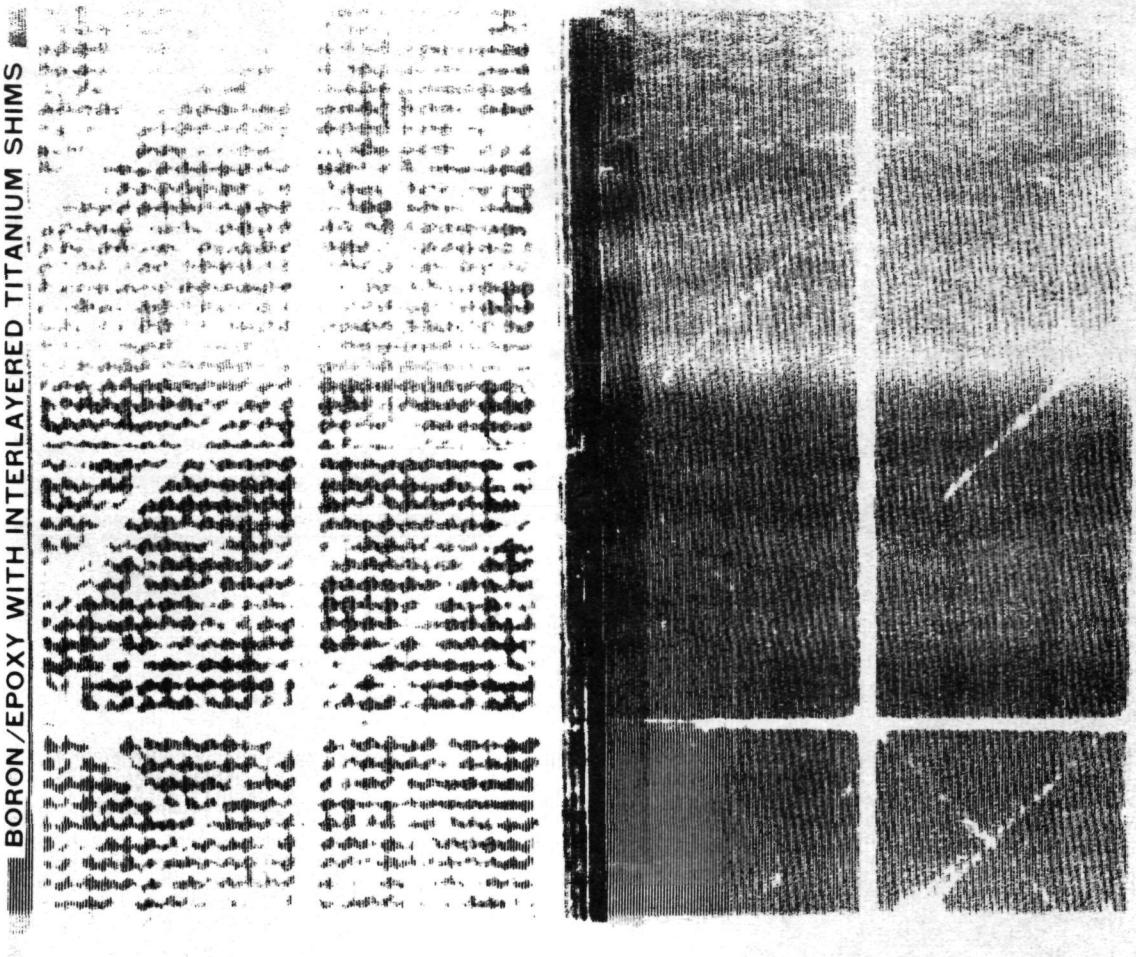

FIGURE 28. ULTRASONIC C-SCAN OF BORON/EPOXY INTERLAYERED TITANIUM SHIM PANEL.

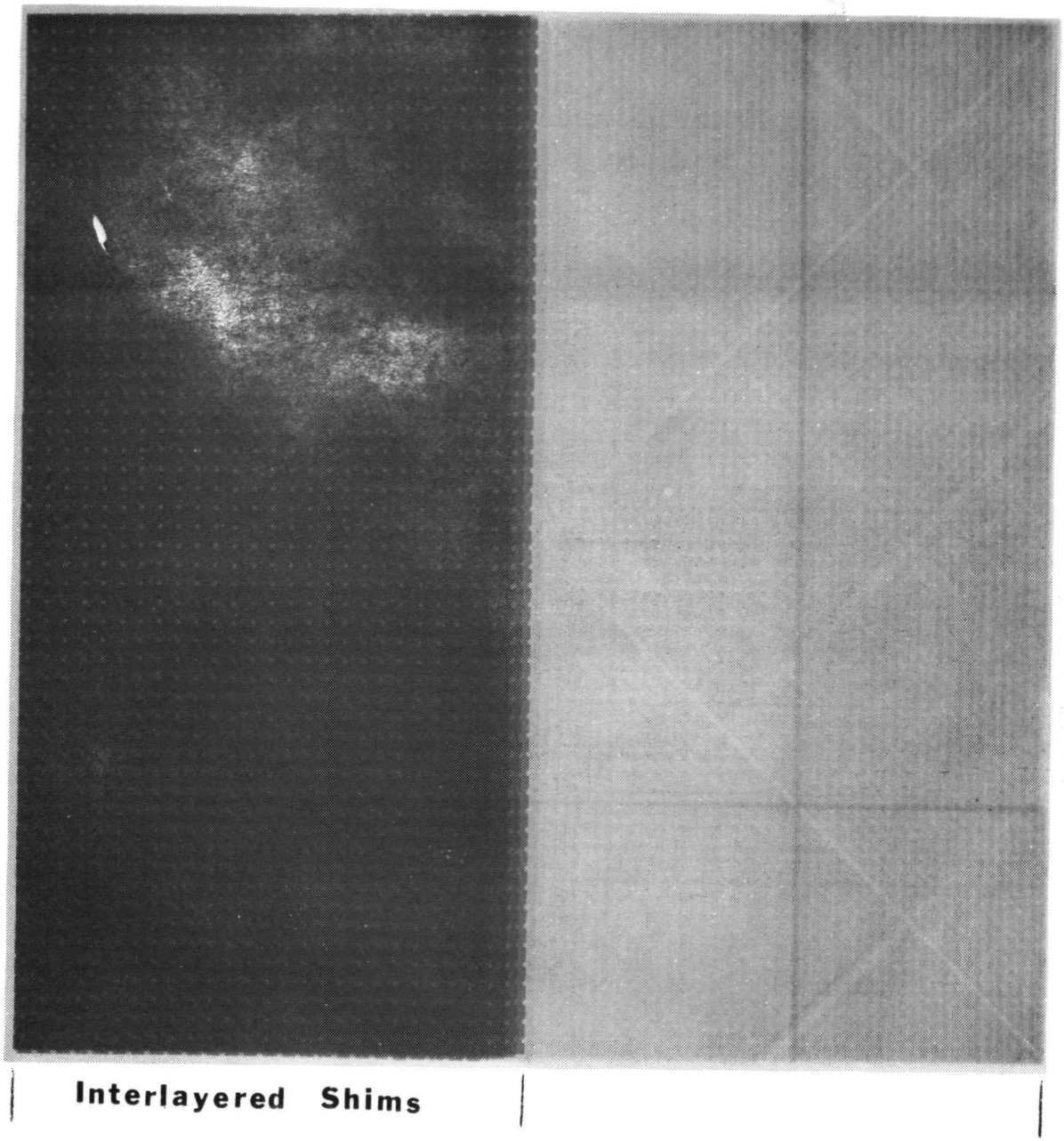

FIGURE 29. RADIOGRAPH OF BORON/EPOXY INTERLAYERED TITANIUM SHIM PANEL. EXPOSURE 2.5 MINUTES.

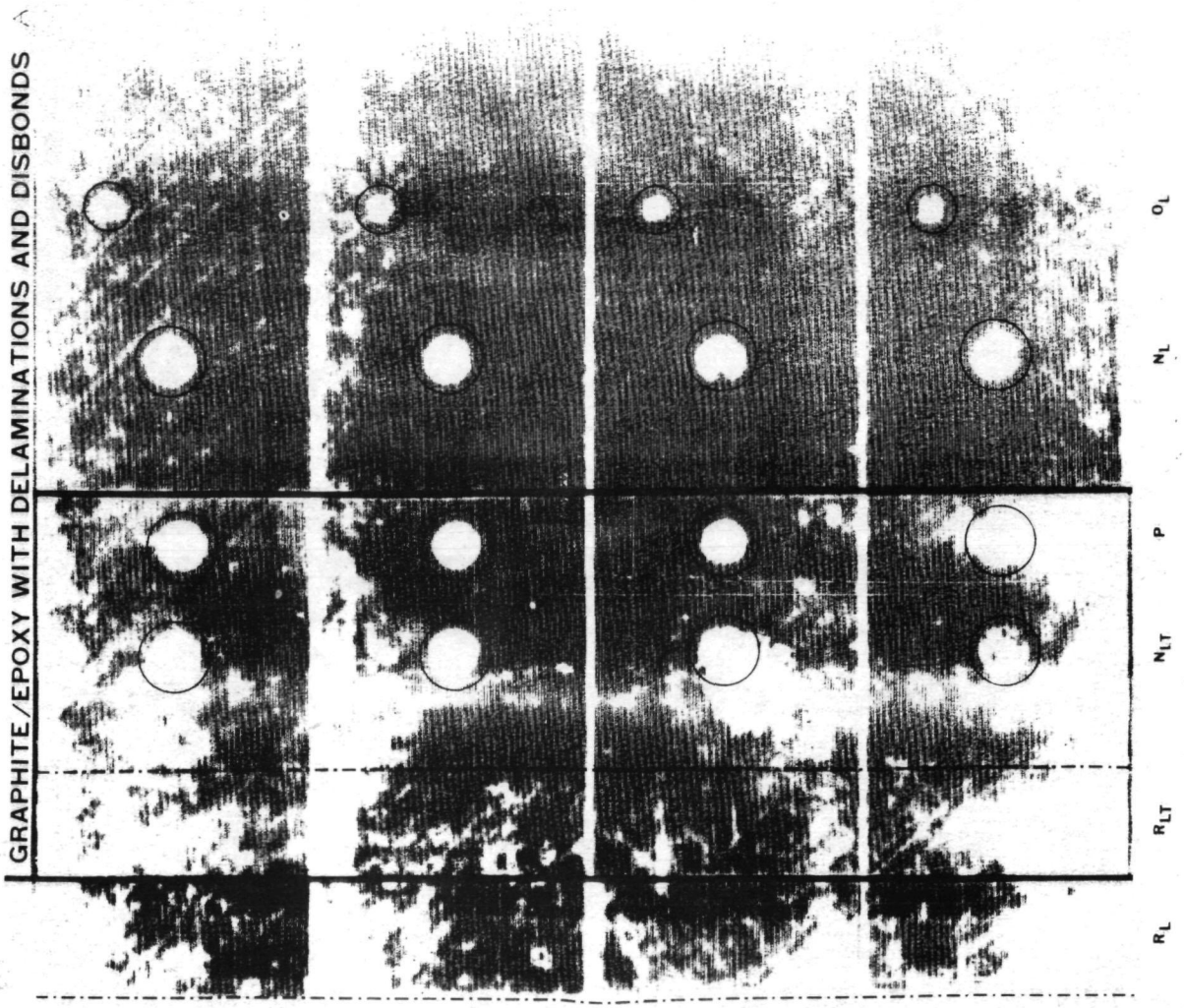

FIGURE 30. ULTRASONIC C-SCAN OF GRAPHITE /EPOXY DELAMINATIONS AND DISBOND PANEL, THICKNESS A.

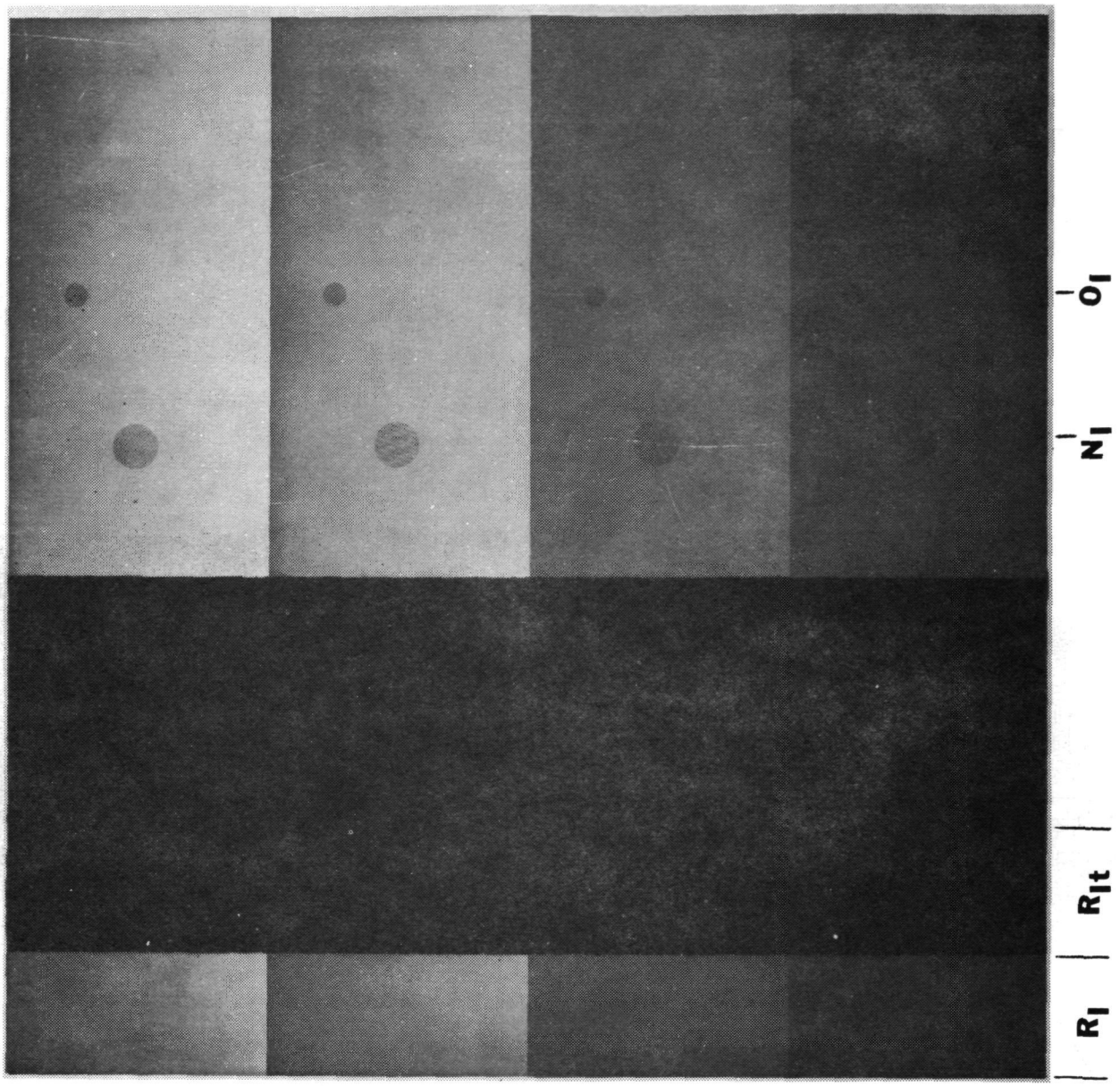

FIGURE 31. RADIOGRAPH OF GRAPHITE/EPOXY DELAMINATIONS AND DISBOND PANEL, THICKNESS A, PLAIN AREAS. EXPOSURE 45 SECONDS.

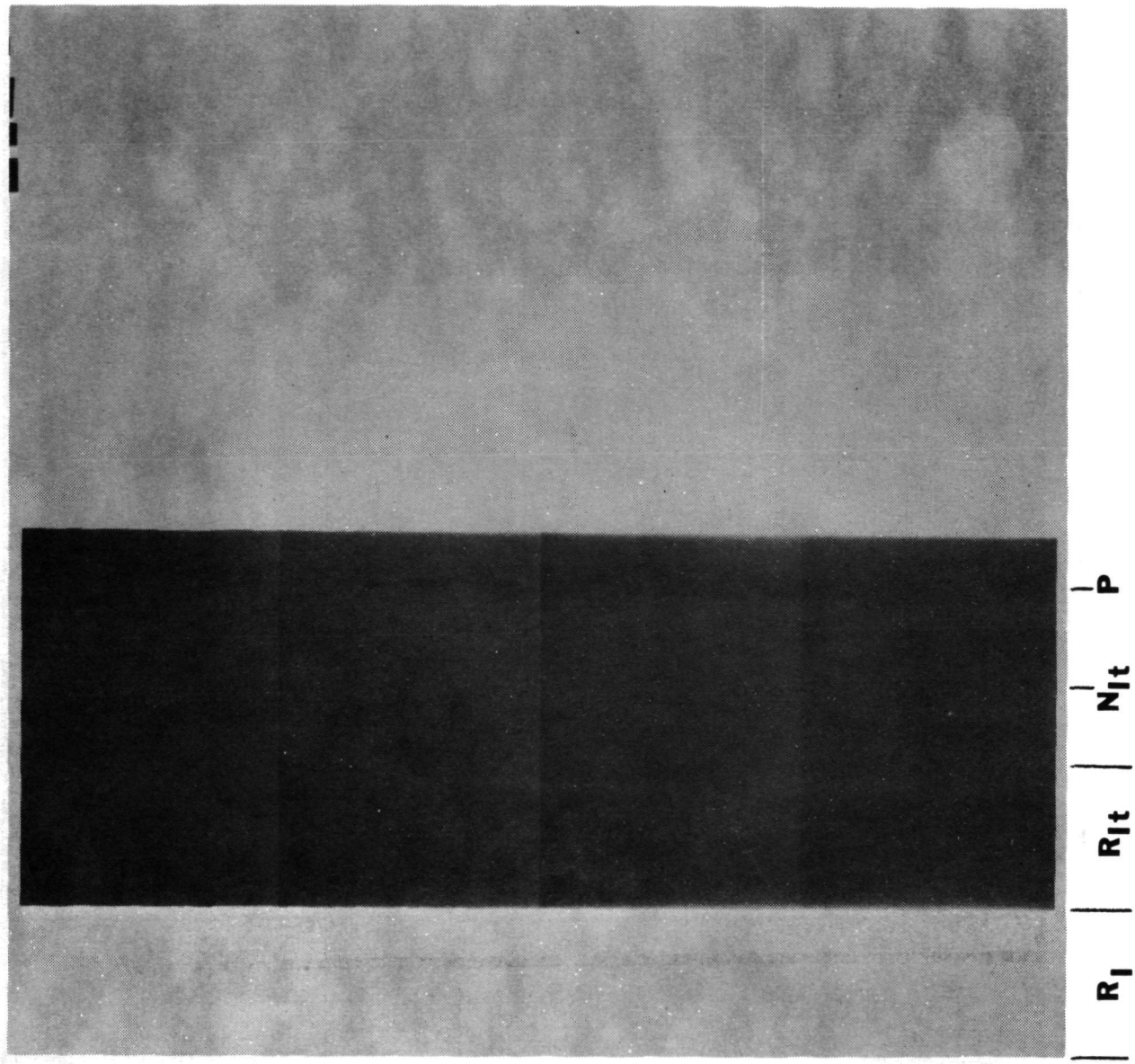

FIGURE 32. RADIOGRAPH OF GRAPHITE/EPOXY DELAMINATIONS AND DISBOND PANEL, THICKNESS A, SUBSTRATE AREAS. EXPOSURE 3 MINUTES.

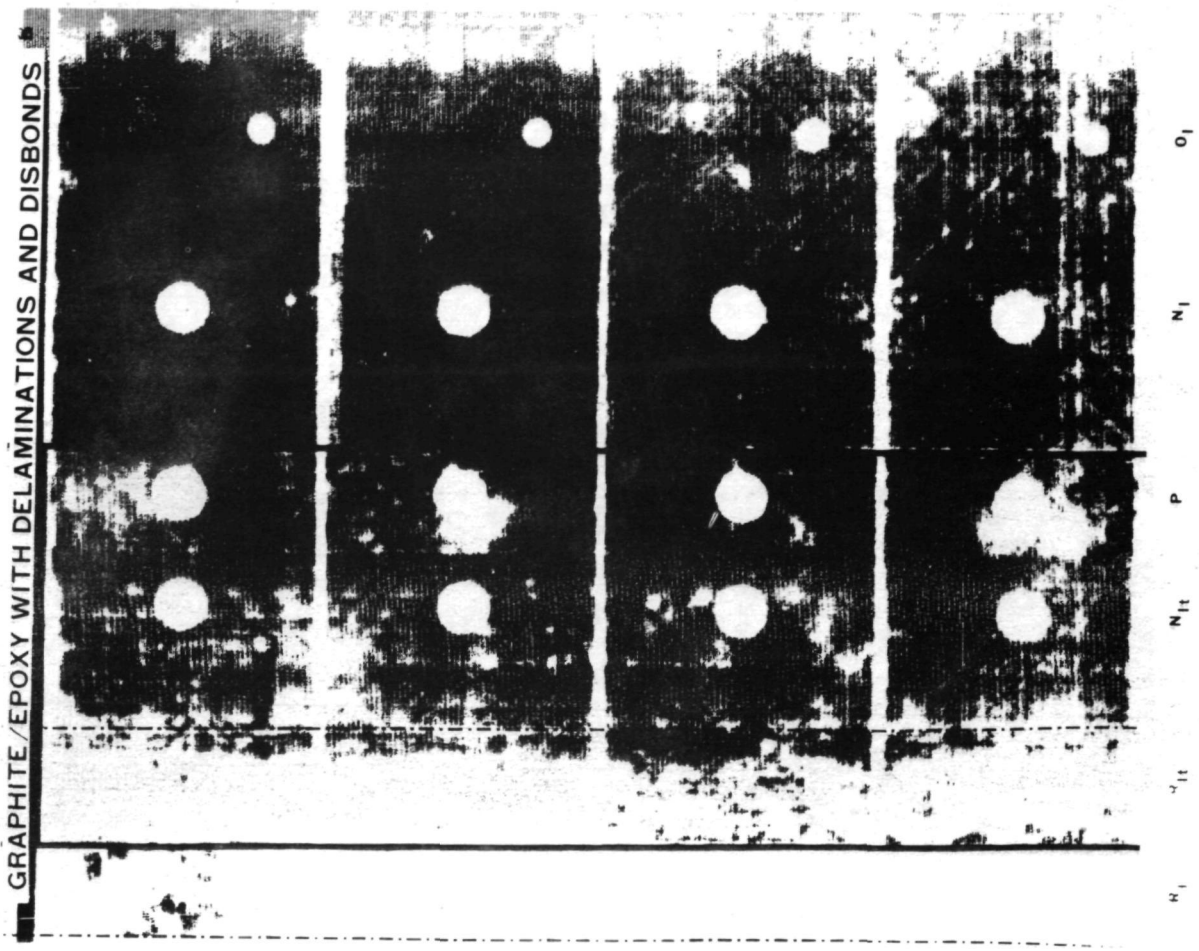

FIGURE 33. ULTRASONIC C-SCAN OF GRAPHITE/EPOXY DELAMINATIONS AND DISBOND PANEL, THICKNESS B.

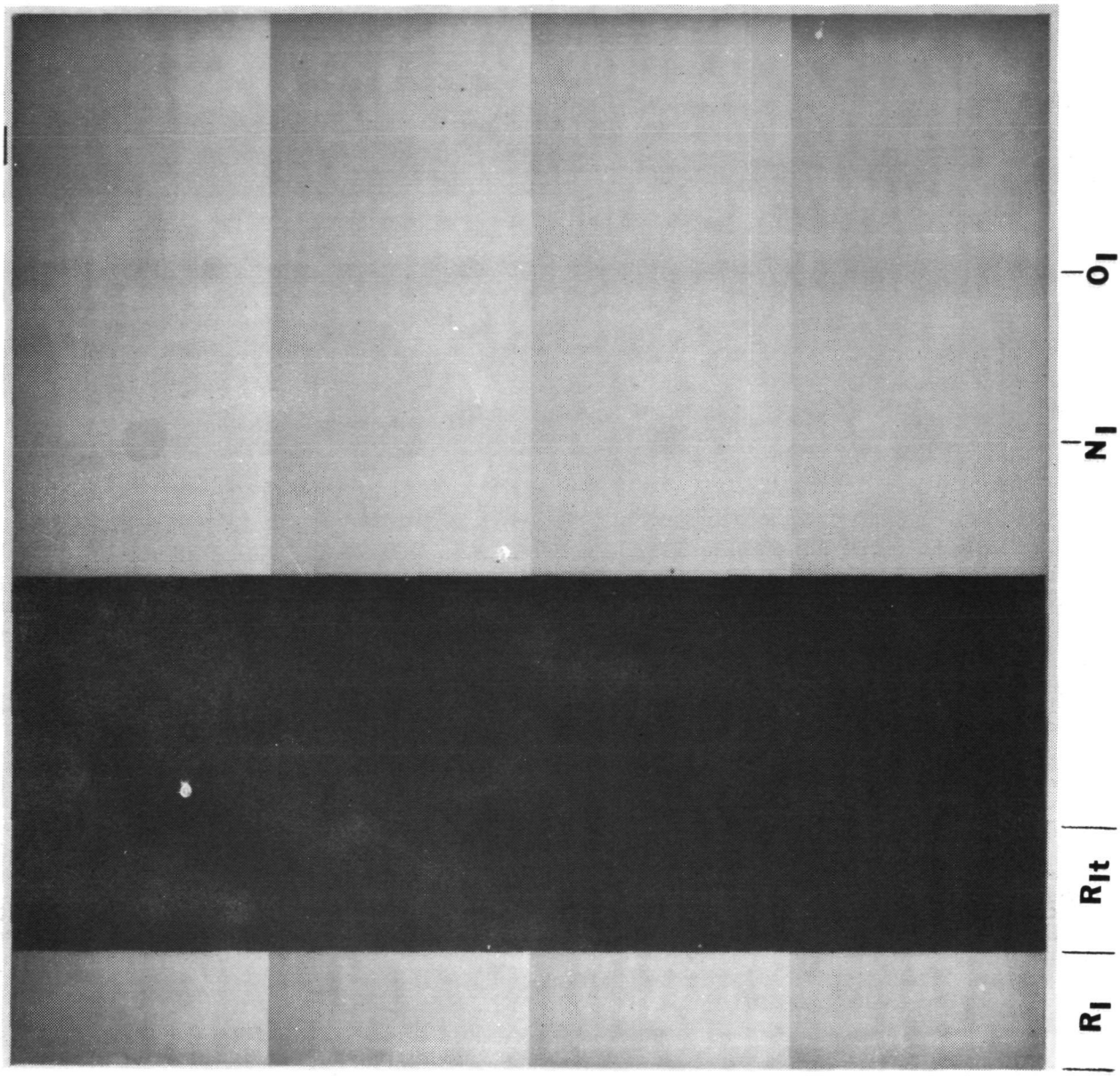

FIGURE 34. RADIOGRAPH OF GRAPHITE/EPOXY DELAMINATIONS AND DISBONDS PANEL, THICKNESS B, PLAIN AREAS. EXPOSURE 60 SECONDS.

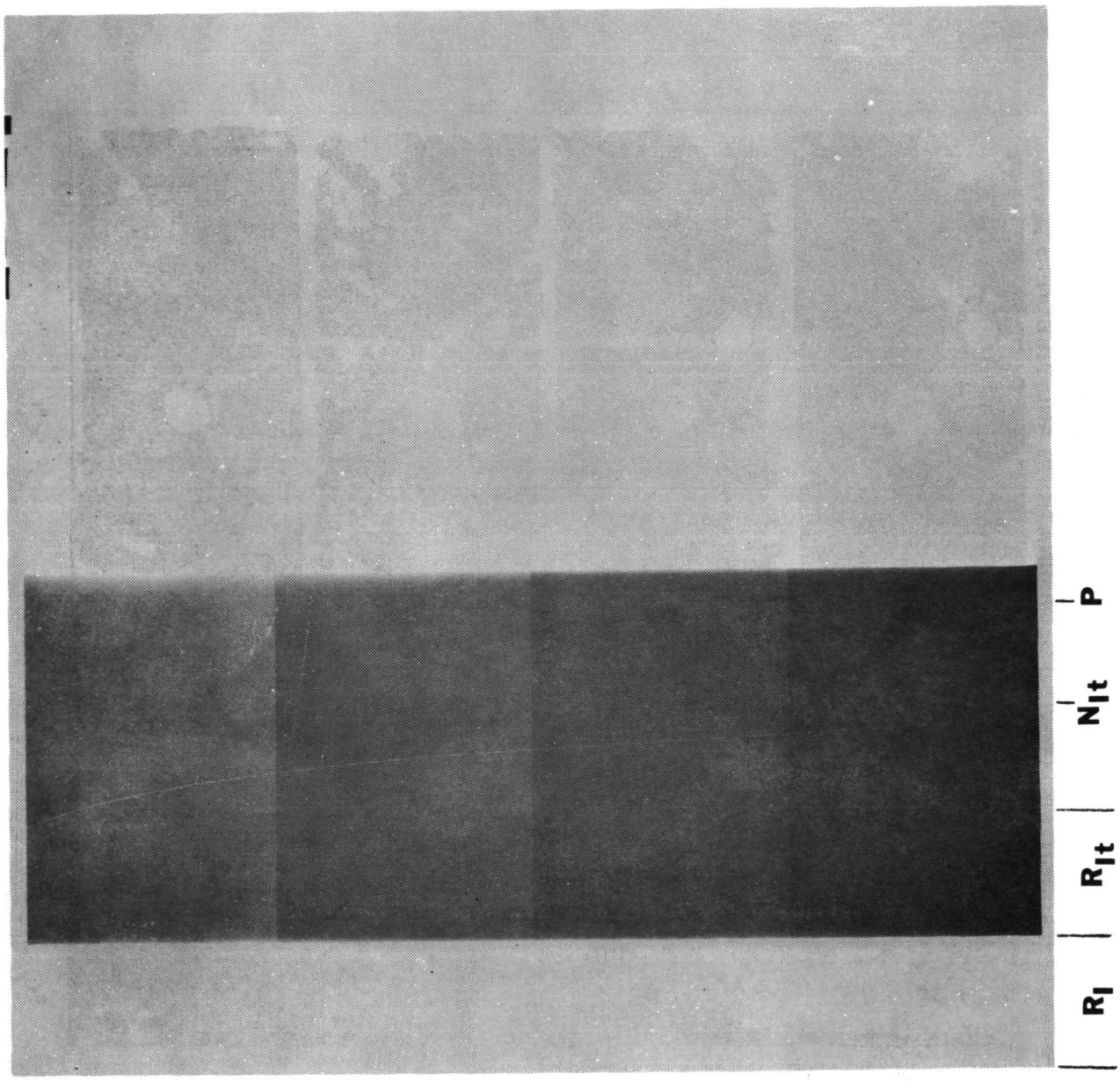

FIGURE 35. RADIOGRAPH OF GRAPHITE/EPOXY DELAMINATIONS AND DISBONDS PANEL, THICKNESS B, SUBSTRATE AREAS. EXPOSURE 3 MINUTES.

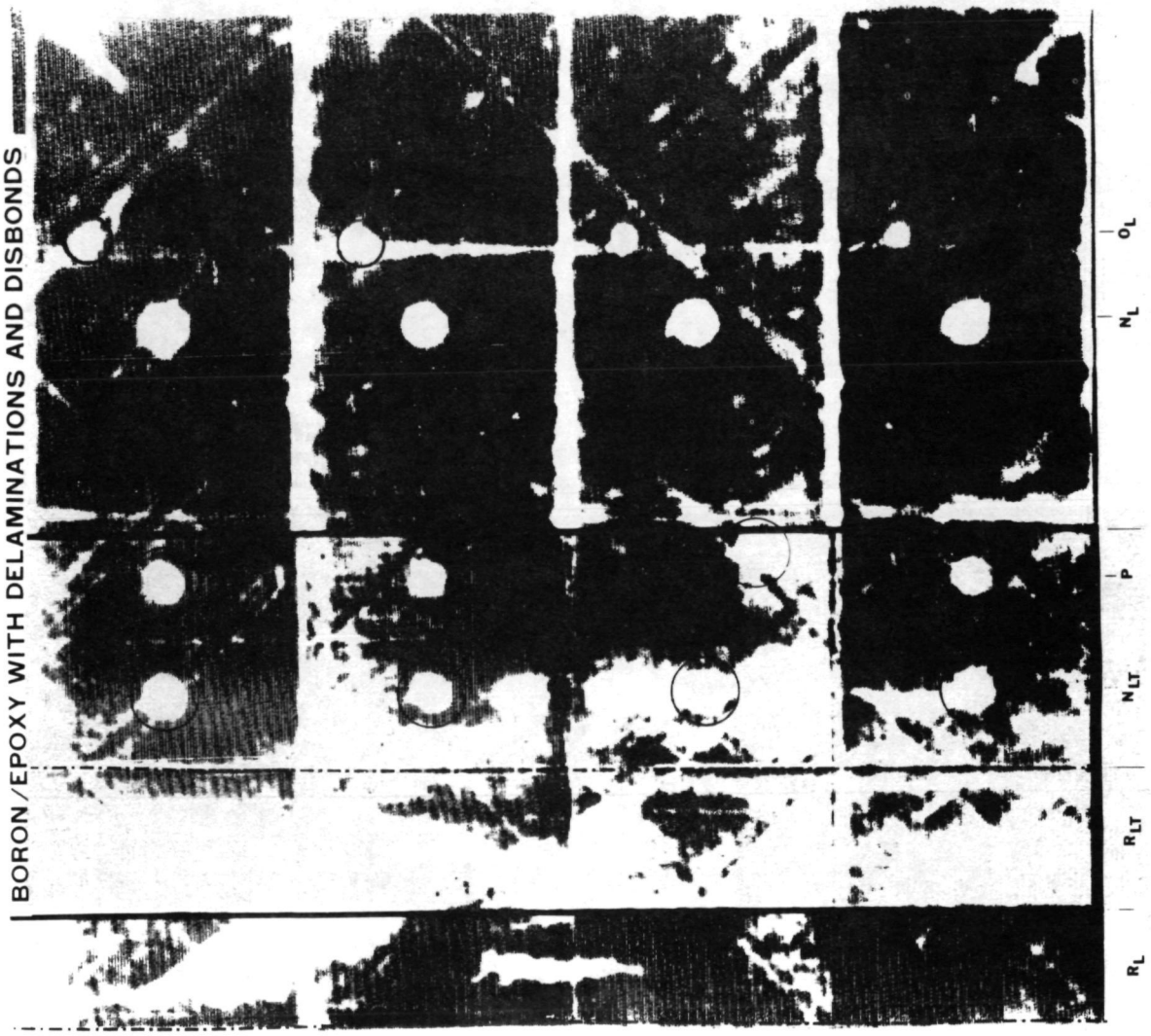

FIGURE 36. ULTRASONIC C-SCAN OF BORON/EPOXY DELAMINATIONS AND DISBONDS PANEL.

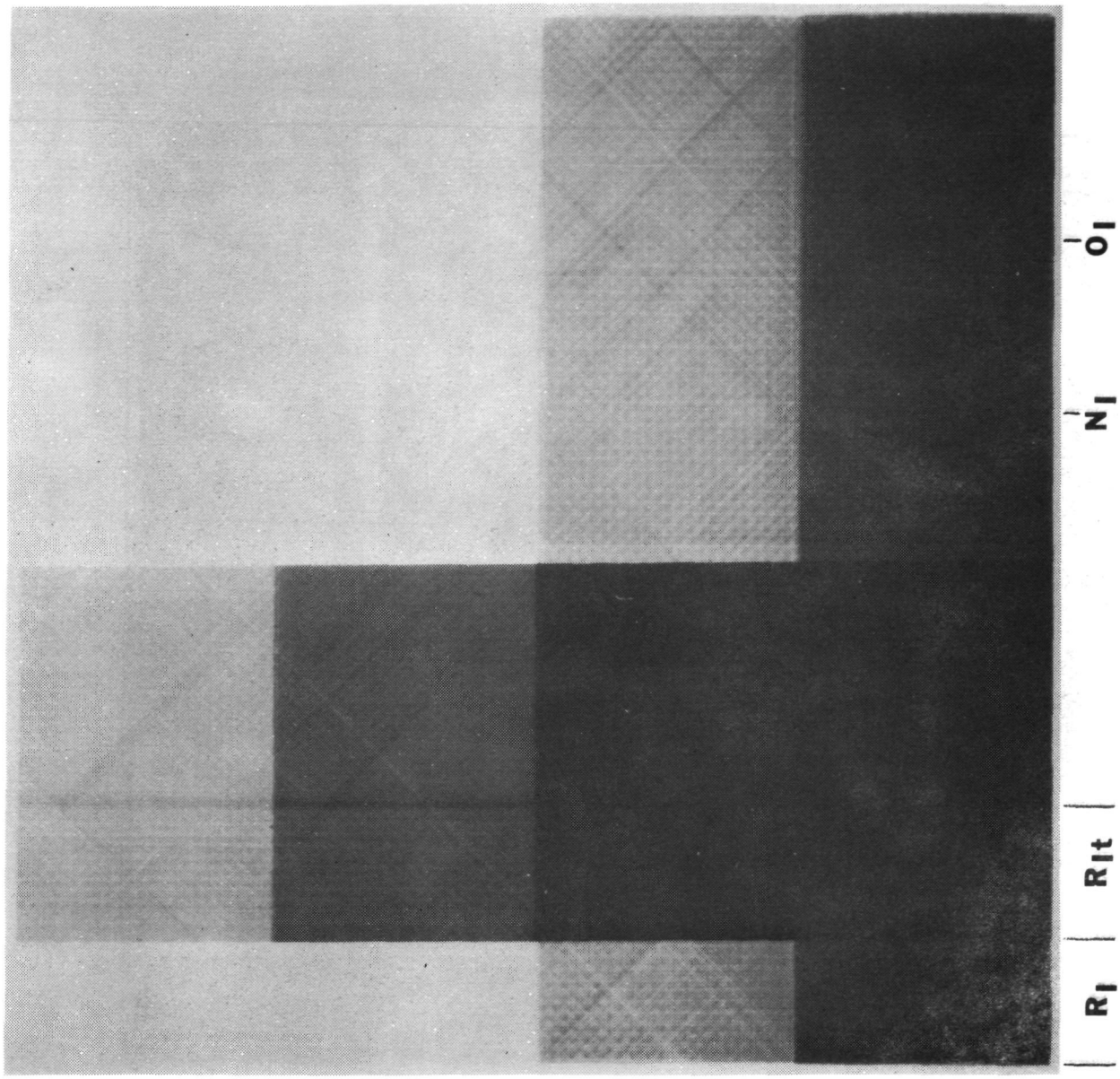

FIGURE 37. RADIOGRAPH OF BORON/EPOXY DELAMINATIONS AND DISBONDS PANEL, PLAIN AREAS. EXPOSURE 2.5 MINUTES.

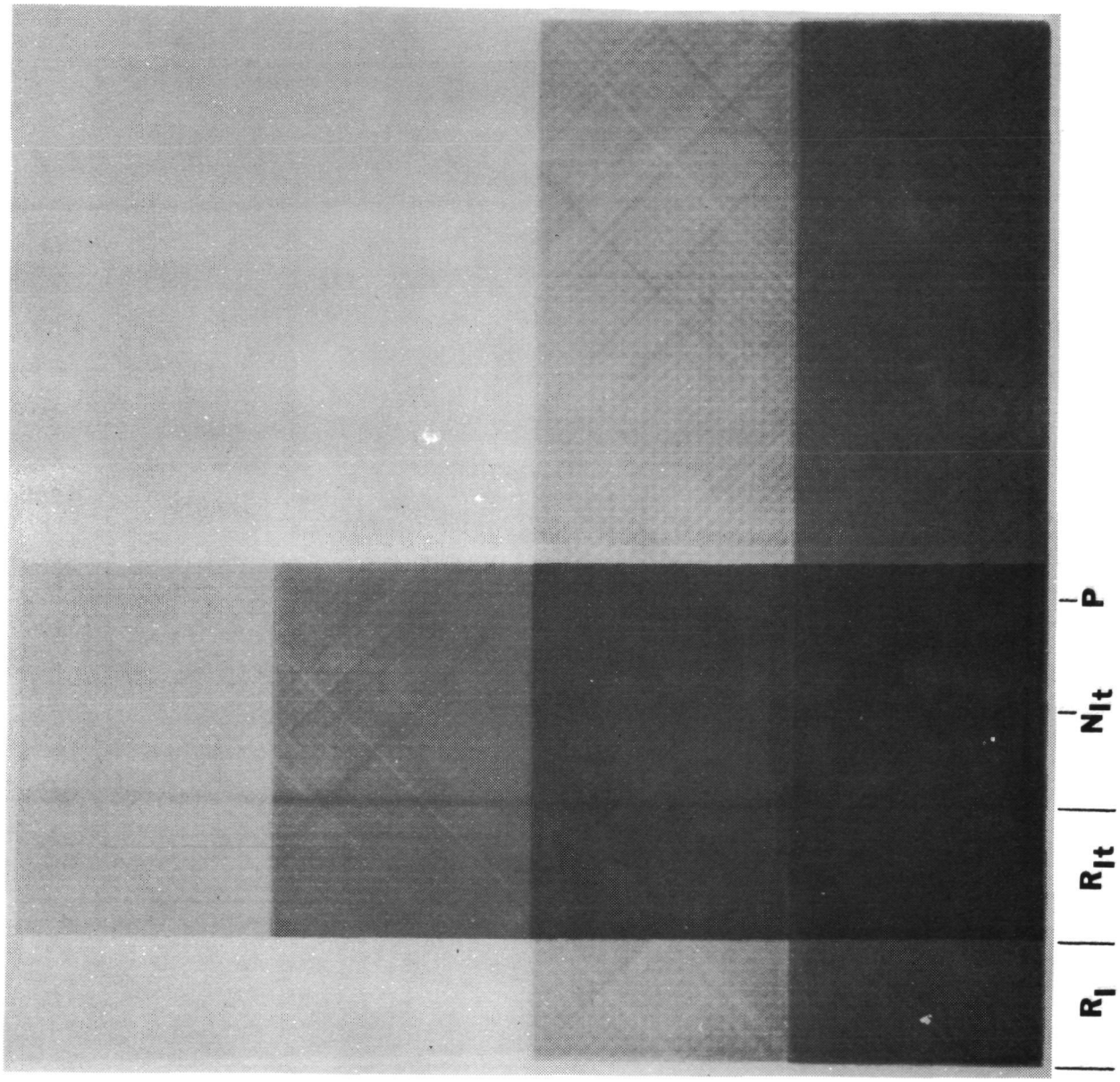

FIGURE 38. RADIOGRAPH OF BORON/EPOXY DELAMINATIONS AND DISBONDS PANEL, SUBSTRATE AREAS. EXPOSURE 5 MINUTES.

APPENDIX

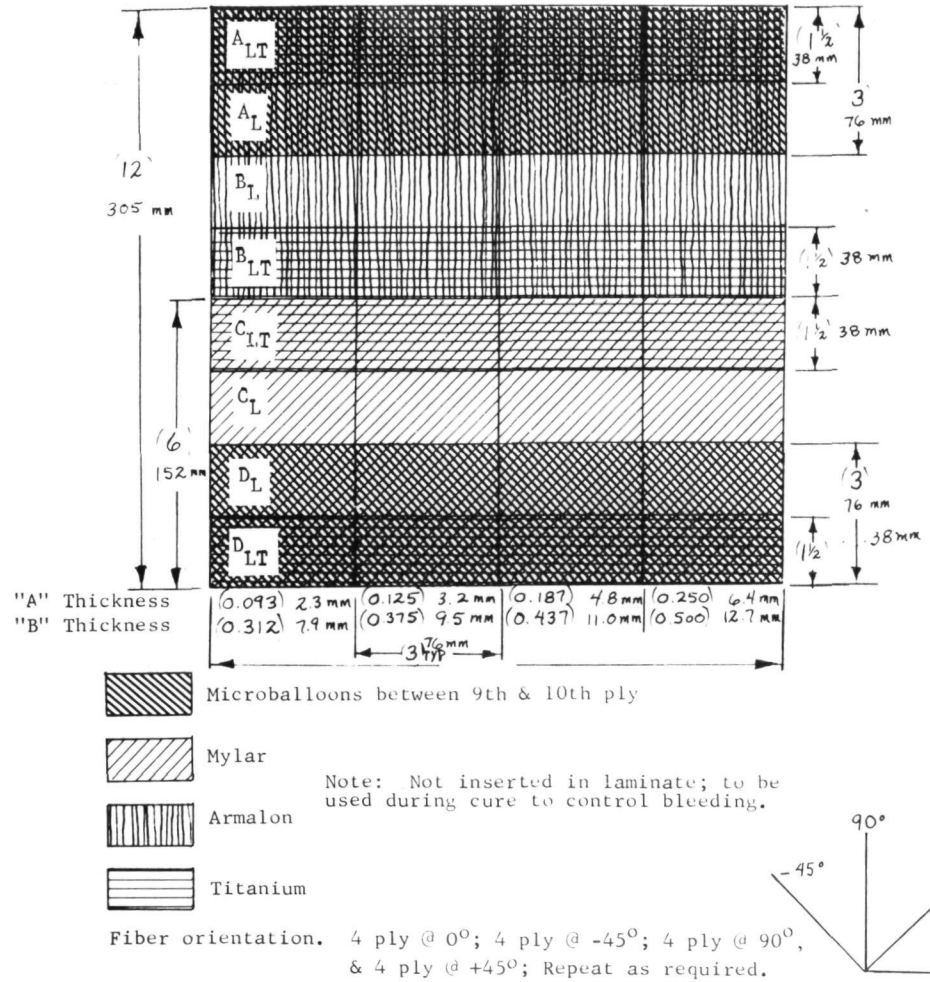

A_L - Plain laminate with porosity, low density, and low r/f ratio.

A_{LT} - With titanium

B_L - Plain laminate with low r/f ratio.

B_{LT} - With titanium

C_L - Plain laminate with high r/f ratio.

C_{LT} - With titanium

D_L - Plain laminate with porosity, low density, and high r/f ratio.

D_{LT} - With titanium

Make one boron/epoxy panel thickness "A" and one thickness "B".

Make one graphite/epoxy panel thickness "A" and one thickness "B".

Bond titanium panels to all four as shown.

FIGURE A-1. DESIGN DRAWING OF THE POROSITY/DENSITY AND RESIN VARIATIONS PANELS.

FIGURE A-2. DESIGN DRAWING OF THE CURE VARIATIONS AND INCLUSIONS PANELS.

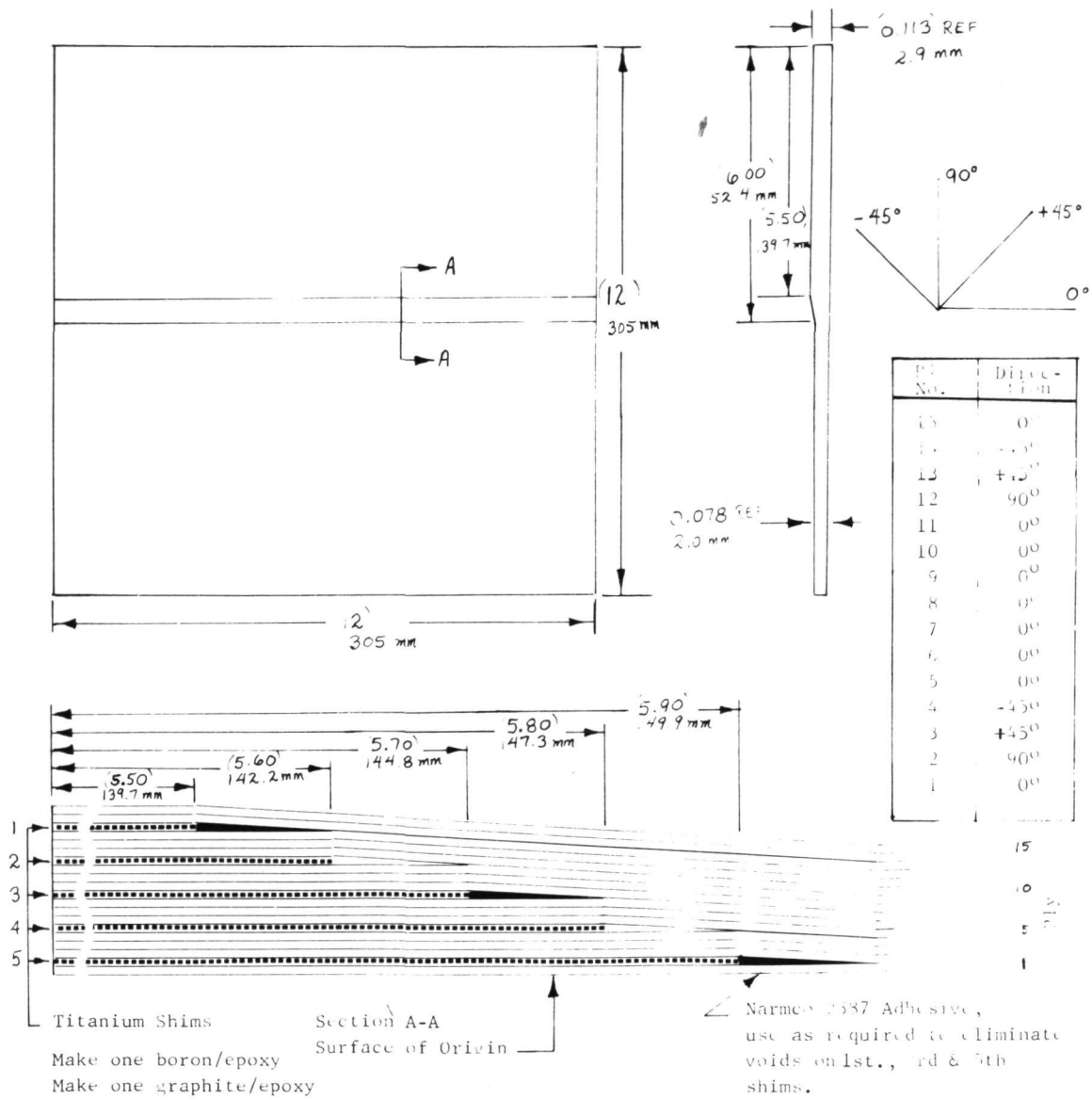

FIGURE A-3. DESIGN DRAWING OF THE INTERLAYERED SHIM PANELS.

Make from annealed Ti-6Al-4V Type III per MIL-T-9046, or equivalent.

All dimensions in inches unless noted.

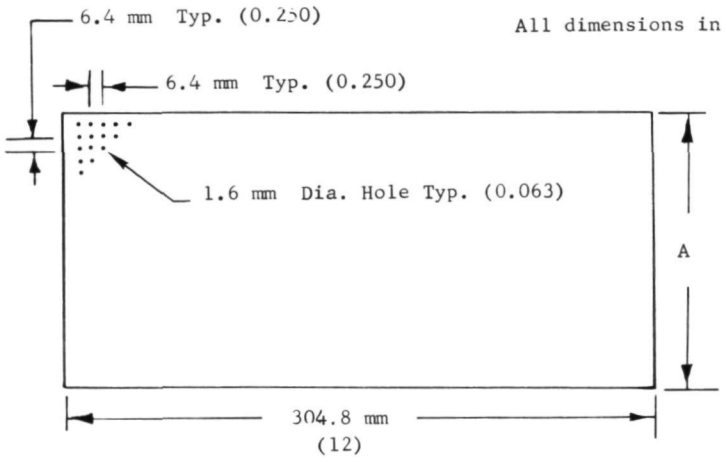

No. Req'd.	Dim. A
2	139.7 mm (5.50)
2	142.2 mm (5.60)
2	144.8 mm (5.70)
2	147.3 mm (5.80)
2	149.9 mm (5.90)

FIGURE A-4. DESIGN DRAWING OF THE TITANIUM SHIMS.

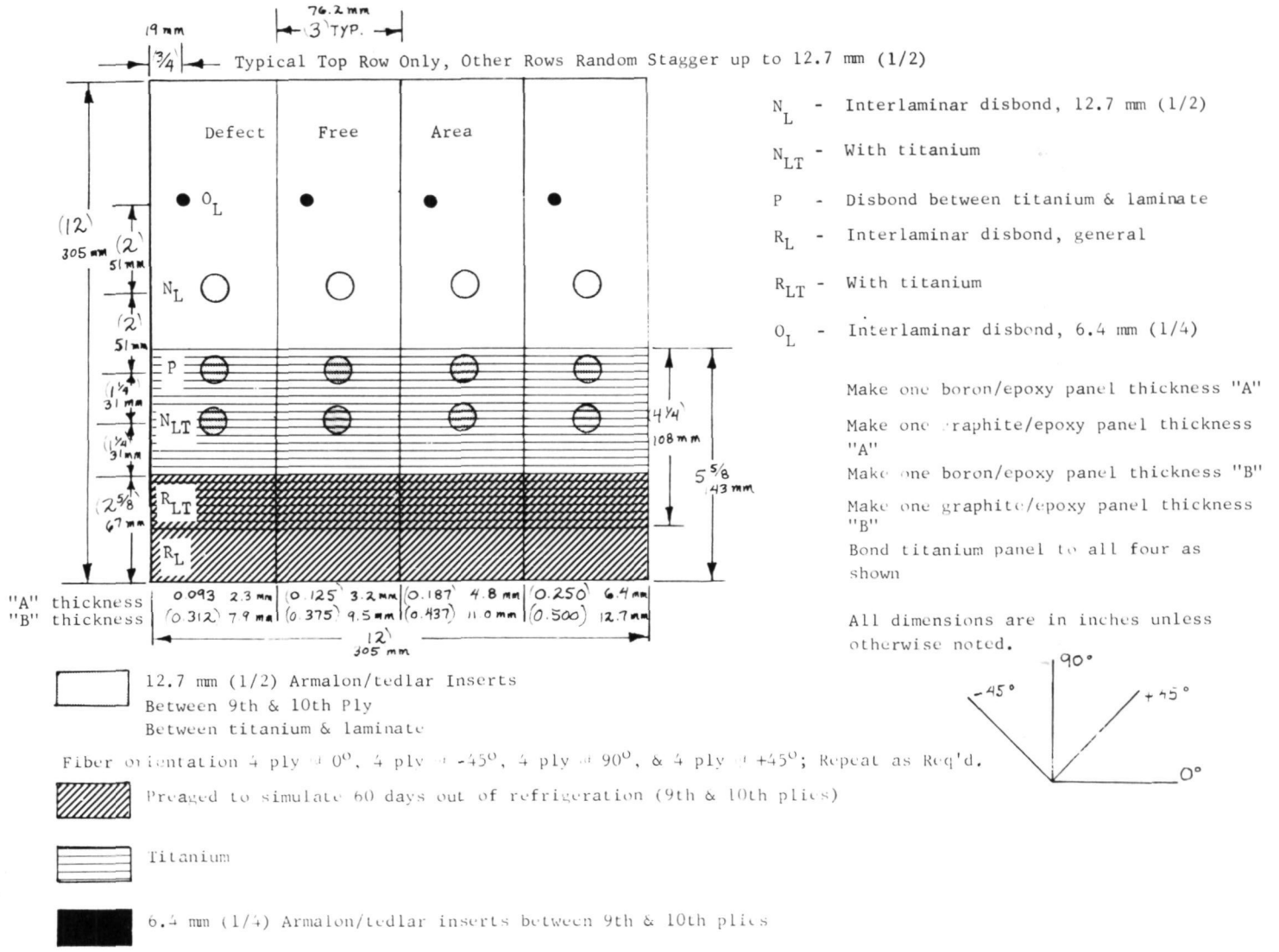

FIGURE A-5. DESIGN DRAWING OF THE DELAMINATIONS AND DISBONDS PANELS.

FIGURE A-6. PHOTOGRAPH OF THE ULTRASONIC C-SCAN SYSTEM.

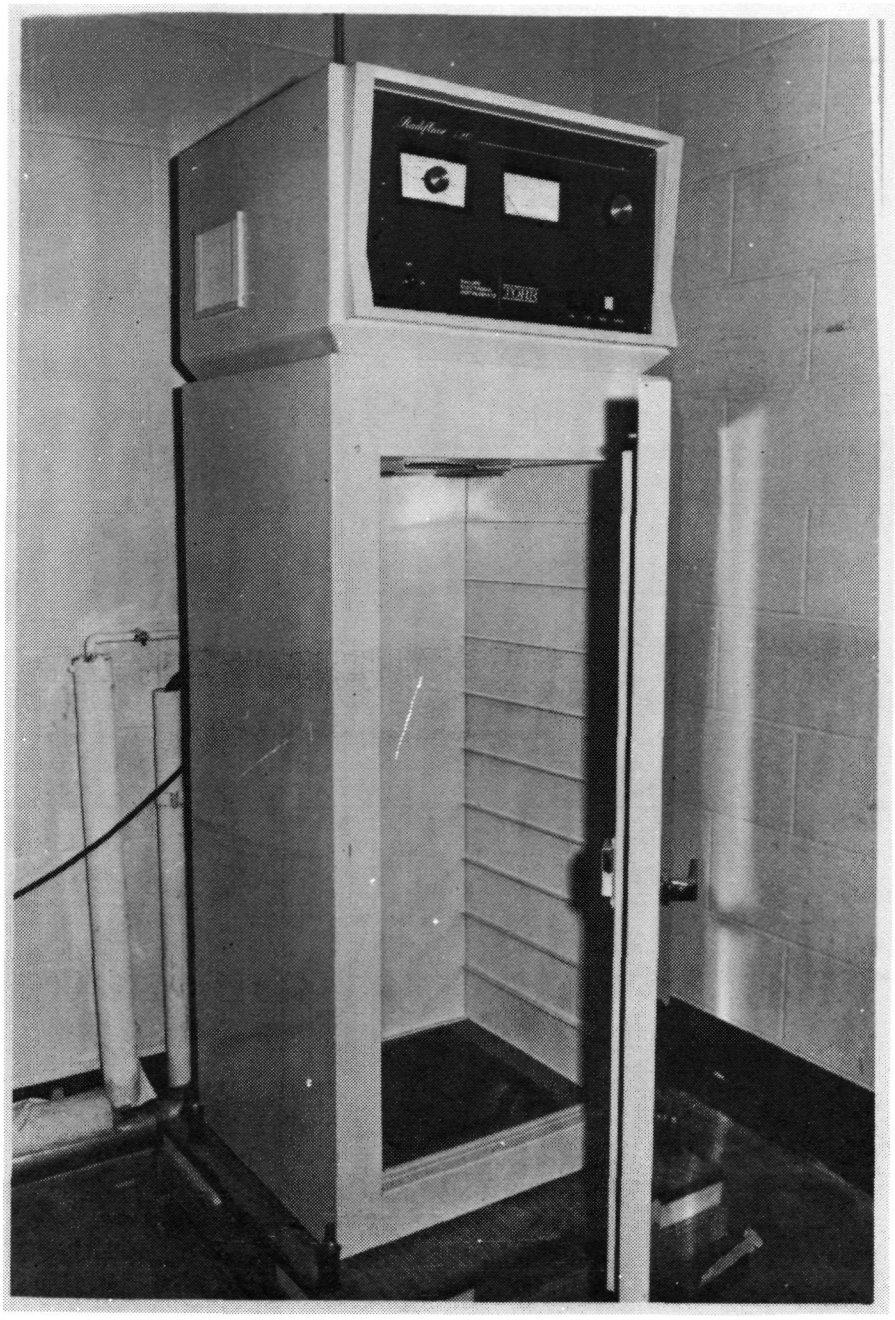

FIGURE A-7. PHOTOGRAPH OF THE RADIFLUOR X-RAY CABINET.

☆ U. S. GOVERNMENT PRINTING OFFICE: 1972 — 745-382 / 4064, REGION NO. 4